JRC Scientific and Technical Reports

JRC Ispra EMEP – GAW regional station for atmospheric research

2005 report

Jean-Philippe Putaud, Fabrizia Cavalli, Alessandro Dell'Acqua, and Sebastiao Martins Dos Santos

Institute for Environment and Sustainability

JRC
EUROPEAN COMMISSION

ies
Institute for
Environment and
Sustainability

EUR 22869 EN – 2007

The mission of the Institute for Environment and Sustainability is to provide scientific-technical support to the European Union's Policies for the protection and sustainable development of the European and global environment.

European Commission
Joint Research Centre

Contact information
J.-P. Putaud
Joint Research Centre
Institute for Environment and Sustainability
TP 290
I-21020 Ispra (Va), Italy

jean.putaud@jrc.it

Tel.: +390332785041
Fax: +390332785837

http://ccu.jrc.it/

http://www.jrc.ec.europa.eu

A great deal of additional information on the European Union is available on the Internet.
It can be accessed through the Europa server
http://europa.eu/

JRC Ispra EMEP – GAW regional station for atmospheric research

2005 report

Jean-Philippe Putaud, Fabrizia Cavalli, Alessandro Dell'Acqua, and Sebastiao Martins Dos Santos
Institute for Environment and Sustainability

Introduction

Location

The JRC station for atmospheric research (45°48.881'N, 8°38.165'E, 209 m asl) is located by the Northern fence of the JRC-Ispra site, situated in a semi-rural area at the NW edge of the Po valley. The station is several tens of km away from large emission sources like intense road traffic or big factories. The main cities around are Varese, 20 km east, Novara, 40 km south, Gallarate - Busto Arsizio, about 20 km south-east and the Milan conurbation, 60 km to the south-east. Busy roads and highways link these urban centers. Four industrial large source points (CO emissions > 1000 tons / yr) are located between 20 and 50 km E to SE of Ispra. The closest (20 km SSE) emits also > 2000 tons of NOx per year.

Mission

The aim of the JRC-Ispra station is to monitor the concentration of pollutants in the gas phase, the particulate phase and precipitations, as well as aerosol optical parameters, which can be used for assessing the impact of European policies on air pollution and climate change. Measurements are performed in the framework of international monitoring programs like the *Co-operative program for monitoring and evaluation of the long range transmission of air pollutants in Europe (EMEP)* of the UN-ECE Convention on Long-Range Transboundary Air Pollution *(CLRTAP)* and the *Global Atmospheric Watch (GAW)* Program of the World Meteorological Organization (WMO).

The EMEP program (http://www.emep.int/)

Currently, 50 countries and the European Community have ratified the CLRTAP. Lists of participating institutions and monitoring stations (Fig. 1) can be found at: http://www.nilu.no/projects/ccc/network.html.

The set-up and running of the JRC-Ispra EMEP station resulted from a proposal of the Directorate General for Environment of the European Commission in Brussels, in agreement with the Joint Research Centre, following the Council Resolution N° 81/462/EEC, article 9. The JRC-Ispra station operates on a regular basis in the extended EMEP measurement program since November 1985. Data are transmitted yearly to the EMEP Chemical Coordinating Centre (CCC) for data control and statistical evaluation.
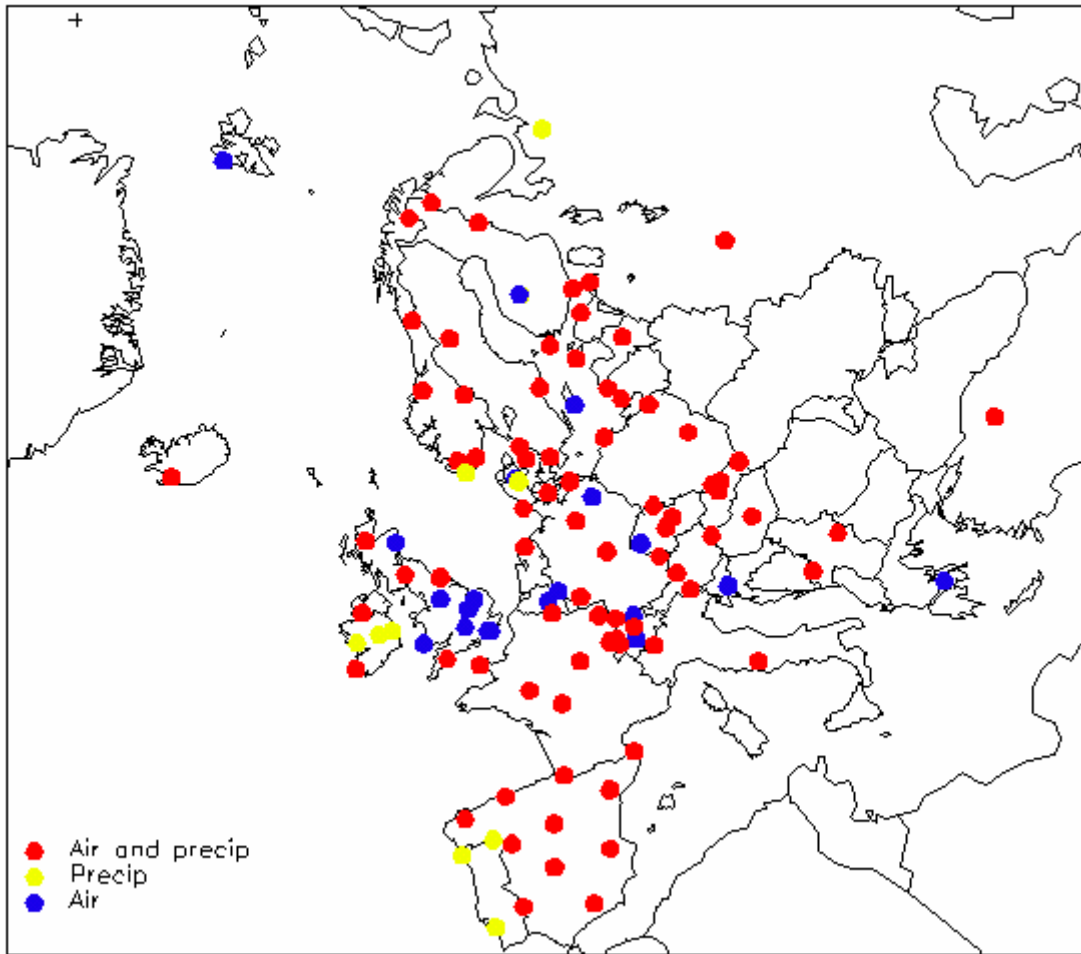
Fig. 1: The EMEP sites in 2001

The GAW program (http://www.wmo.int/web/arep/gaw/gaw_home.html)

WMO's Global Atmospheric Watch (GAW) system was established in 1989 with the scope of providing information on the physico-chemical composition of the atmosphere. These data provide a basis to improve our understanding of both atmospheric changes and atmosphere-biosphere interactions. GAW is one of WMO's most important contributions to the study of environmental issues, with about 80 member countries participating in GAW's measurement program. Since December 1999, the JRC-Ispra station is also part of the GAW coordinated network of regional stations. Aerosol data submitted to EMEP are to automatically flow to the GAW World Data Center for Aerosol (WDCA), hosted by the JRC-IES Climate Change Unit.

The institutional program (http://ccu.jrc.it/)

The JRC-Ispra station has been managed by the Climate Change Unit of the European Commission - Joint Research Centre (JRC) Institute for Environment and Sustainability since February 2002. From then its monitoring program has been focused on air pollution and climate forcing short-lived agents such as tropospheric ozone and aerosols. Concretely, more sensitive gas monitors were introduced, as well as a set of new measurements providing aerosol characteristics that are linked to its radiative forcing.

The site was also used for research and development purposes, mainly focusing on organic carbon sampling artifacts. The data obtained in Ispra are being used for the design of the new EMEP monitoring strategy and the revision of the EMEP sampling and analytical procedure manual.

JRC-Ispra station data are available on-line at http://airispra.jrc.it/Start.cfm or from the IES web site http://ies.jrc.cec.eu.int/. Historical data can also be downloaded from the Climate Change Unit web page by selecting Data Sets and then **EMEP station data.**
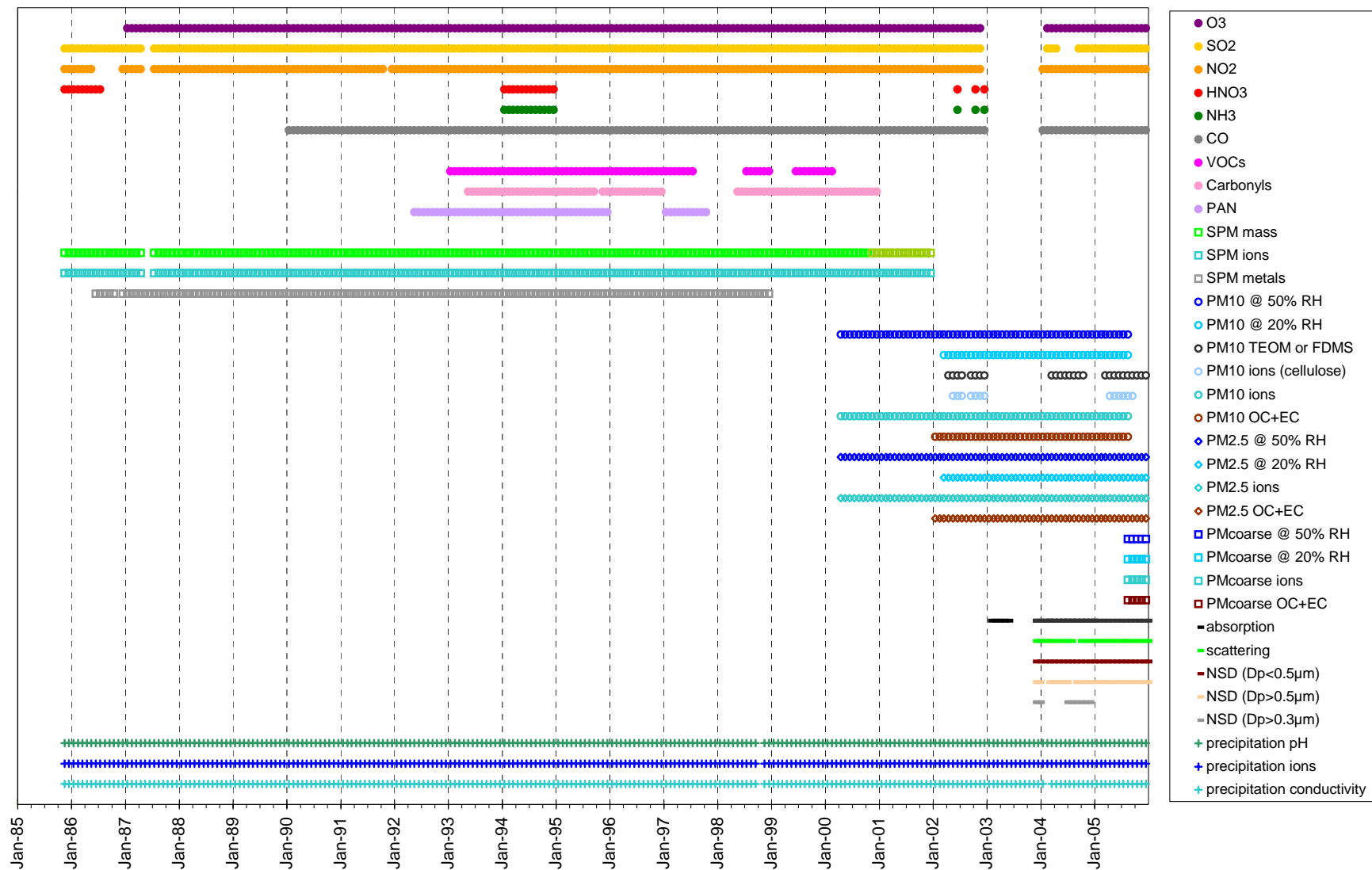
Fig. 2: measurements performed at the JRC-Ispra station for atmospheric research since 1985

The JRC-Ispra station for atmospheric research measurement program

Since 1985, the JRC-Ispra air monitoring station program evolved significantly (Fig. 2). The parameters measured at the JRC-Ispra station in 2005 are listed in Table 1. Meteorological parameters were not measured at the station in 2005. The meteorological data used in this report were collected at surrounding station, at Bd. 51 and Malpensa airport (see Figure 7 for specifications). Figure 3 shows the data coverage for 2005. NOx, O_3 and CO were measured over the whole year 2005. SO_2, measurements were resumed on January 27th, 2005. 24-hr integrated (from 08:00 to 08:00 UTC) particulate matter (PM) samples were collected daily until December 23rd, and analyzed for PM mass (at 20 and 50% RH), main ions, OC and EC. PM_{10} and $PM_{2.5}$ were sampled till July 31st. From July 1st, PM_{coarse} and $PM_{2.5}$ were collected using a single dichotomous sampler. On-line PM10 measurements (FDMS-TEOM) were carried out from March 16th to December 24th, except for short breaks due to technical problems or maintenance. Aerosol absorption coefficient and particle number size distribution (Dp < 500 nm) were measured continuously over the whole year. Particle number size distribution (Dp > 500 nm), and scattering coefficient were measured continuously over 2005, except from Sept. 9th to Oct. 12th and in December, and from Sept. 8th to Oct. 21st, respectively. Precipitation was collected throughout the year and analyzed for pH, conductivity, and main ions.

Table 1: parameters measured during 2003-2004

GAS PHASE	SO_2, NO, NO_X, O_3, CO
PARTICULATE PHASE	In two size fractions, PM mass and Cl^-, NO_3^-, SO_4^{2-}, $C_2O_4^{2-}$, Na^+, NH_4^+, K^+, Mg^{2+}, Ca^{2+}, OC, and EC
	Number size distribution (10 nm - 10 μm)
	Aerosol absorption, scattering and back-scattering coeff.
PRECIPITATION PHASE	Cl^-, NO_3^-, SO_4^{2-}, $C_2O_4^{2-}$, Na^+, NH_4^+, K^+, Mg^{2+}, Ca^{2+} pH, conductivity

Fig. 3: 2005 data capture

Fig. 4. Schematic diagram of GFC monitor for CO. A = optical layout (M denotes mirror reflector, and L denotes lens); B = detail of correlation cell. Source: Chaney and McClenny (1977).

The JRC-Ispra station for atmospheric research measurement techniques

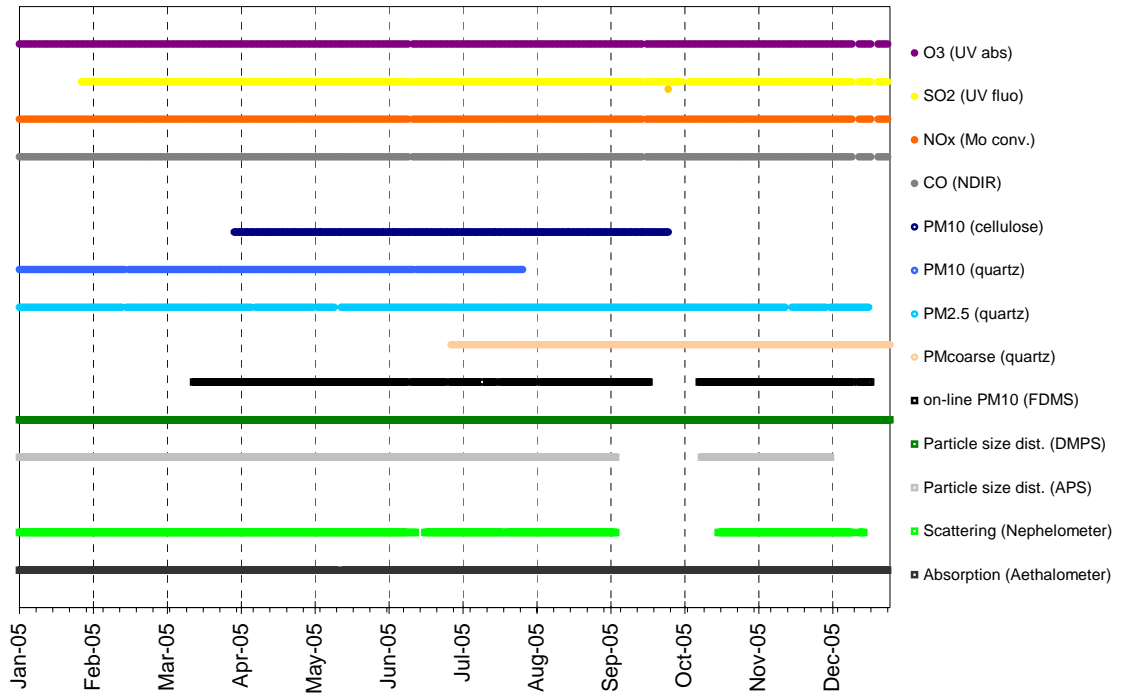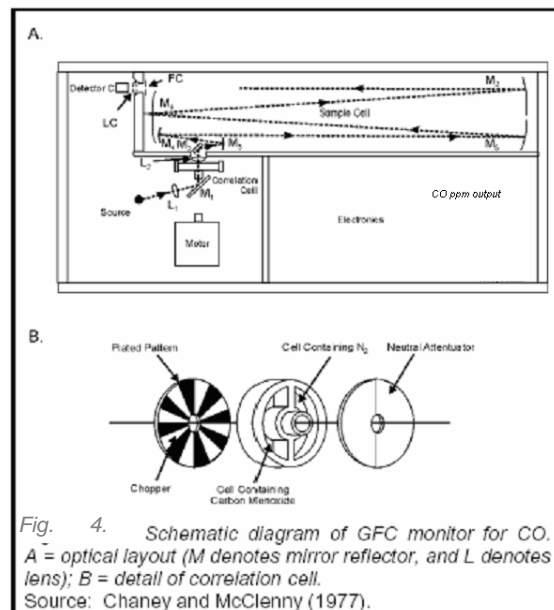## On-line Monitoring

Meteorological Parameters

No meteorological parameters were monitored at the station over 2005. Meteorological data acquired at Bd 51 (ca. few 1500 m south-west of the station) are reported instead. When data were lacking, we used the meteorological data monitored at Malpensa airport, 20 km south-east of the station.

Gaseous Air Pollutants

Sampling

Gases are sampled from a common inlet situated at 3.5m above the ground on the roof of the gas monitors' container. The sampling line consists in an inlet made of a PVC semi-spherical cap (to prevent rain and bugs enter the line), a PTFE tube (Ø=2.54 cm, h=150 cm), the lower part of which is kept at 60 (±10) °C, and a "multi-channel distributor" glass tube kept at 40 (±10) °C (by internal heating), with nine 14mm lateral threaded connectors. This inlet is flushed by a 34 L/min flow (*measured with RITTEWR 11456 on 23/07/04*). Each instrument samples from the glass tube with its own pump through a ¼" Teflon line and a 1 µm pore size 47 mm diameter Teflon filter (to eliminate particles from the sampled air).

Gas monitors are calibrated 7-11 times a year. Sampling flow rates are as follow:

Analyte	L/min
CO	1.6
SO_2	0.5
NO, NO_2, NO_x	0.6
O_3	2.0

CO: *Non-Dispersive Infrared Gas-Filter Correlation Spectroscopy*

TEI 48C-TL (60873-328)

A *Gas-Filter Correlation (*GFC) monitor (Burch et al., 1976) has the advantages of a NDIR instrument: no interference from CO_2, and very small interference from water vapor. A top schematic view of the GFC monitor shows the components of the optical path for CO detection (Fig. 4). During operation, air flows continuously through the sample cell. Radiation from the source is directed by optical transfer elements through the two main optical subsystems: (1) the rotating gas filter and (2) the optical multi-path (sample) cell. The beam exits the sample cell through interference filter (FC), which limits the spectral passband to a few of the strongest CO absorption lines in the 4.6-µm region. Detection of the transmitted radiation occurs at the infrared detector. The gas correlation cell is constructed with 4 compartments: 2 compartments are filled with 0.5 atm CO, and the two others are filled with pure N_2. Radiation directed to the CO compartment is completely attenuated at wavelengths where CO absorbs strongly. The radiation transmitted through the N_2 is reduced by coating the exit window of the cell with a neutral attenuator so that the amounts of radiation transmitted by the two cells are made approximately equal in the passband that reaches the detector. In operation, radiation passes alternately through the two cells as they are rotated to establish a signal modulation frequency. If CO is present in the sample, the radiation transmitted through the CO is not appreciably changed, whereas that through the N_2 cell is changed. This imbalance is linearly related to CO concentrations in ambient air.

Calibration is performed monthly using a zero air gas cylinder (Air Liquide, CnHm<0.5 ppm) and an external span gas. The span gas cylinder (160420 & 3514B from Messer Griesheim GmbH) concentrations (8.12 ± 0.07 and 9.199 ± 0.05 ppm, respectively) were

determined at ERLAP (European Reference Laboratory of Air Pollution) in October 2004 and 2005, respectively. The instrument's lower detection limit is 0.02 ppm.

SO$_2$: *UV Fluorescent SO$_2$ Analyser*

AF 21 M-LCD (N° 1693)

At first, the air flow is scrubbed to eliminate aromatic hydrocarbons. The sample is then directed to a chamber where it is irradiated by 214 nm (UV), a wavelength that SO$_2$ molecules absorb. The fluorescence signal emitted by the excited SO$_2$ molecules going back to the ground state is filtered between 300 and 400 nm (specific of SO$_2$) and amplified by a photomultiplier tube. A microprocessor receives the electrical zero and fluorescence reaction intensity signals and calculates SO$_2$ based on a linear calibration curve.

Calibration is performed monthly using a zero air gas cylinder (Air Liquide, CnHm<0.5 ppm) and external span gas cylinders A3489 and 6214F (66 ± 2 ppb). The span gas cylinder (from Messer Griesheim GmbH) concentration were controlled at ERLAP (European Reference Laboratory of Air Pollution) in October 2005.

The specificity of the trace level instrument (TEI 43C-TL) is that it uses a pulsed lamp. The 48C-TL's detection limit is 0.2 ppb (ca. 0.5 μg/m³) according to the technical specifications.

NO + NO$_X$: Chemiluminescent Nitrogen Oxides Analyzer

TEI 42C (A:62581-336 and B: 0401304317)

This nitrogen oxides analyser is based on the principle that nitric oxide (NO) and ozone react to produce excited NO$_2$ molecules, which emit infra-red photons when going back to lower energy states:

$$NO + O_3 \rightarrow NO_2 + O_2 + h\nu$$

A stream of purified air (dried with Drierite™ till July 7th, 2005, with a Nafion Dryer onwards) passing through a silent discharge ozonator generates the ozone concentration needed for the chemiluminescent reaction. The specific luminescence signal intensity is therefore proportional to the NO concentration. A photomultiplier tube amplifies this signal.

NO$_2$ is detected as NO after reduction in a Mo converter heated at about 325°C.

The ambient air sample is drawn into the analyser, flows through a capillary, and then to a valve, which routes the sample either straight to the reaction chamber (NO detection), or through the converter and then to the reaction chamber (NO$_X$ detection). The calculated NO and NO$_X$ concentrations are stored and used to calculate NO$_2$ concentrations, assuming that only NO$_2$ is reduced in the Mo convertor.

Calibration is performed monthly using a zero air gas cylinder (Air Liquide, CnHm<0.5 ppm) and a NO span gas. The NO span gas cylinder MA A 7846 (from Messer Griesheim GmbH) concentration (195.8±1.4 ppb) was controlled in Oct. 2005 at ERLAP (European Reference Laboratory of Air Pollution).

O$_3$: *UV Photometric Ambient Analyzer*

TEI 49C (S/N 55912-305 and 0503110499)

The UV photometer determines ozone concentrations by measuring in the absorption cell the attenuation of UV light (254 nm) due to ozone. The concentration of ozone is related to the magnitude of the attenuation. The reference gas, generated by scrubbing ambient air, passes into one of the two absorption cells to establish a zero light intensity reading, I$_0$. Then the sample passes through the other absorption cell to establish a sample light intensity reading, I. This cycle is reproduced with inverted cells. The average ratio R=I/I$_0$ between 4 consecutive readings is directly related to the ozone concentration in the air

sample through the Beer-Lambert law. Instrument S/N was added on Nov. 25th, 2005, and used as primary instrument (reported on-line and to EMEP) since then.

Calibration is performed monthly using externally generated zero air and external span gas. Zero air is taken from a gas cylinder (Air Liquide, CnHm < 0.5 ppm). Span gas (50ppb in winter and 100ppb in summer and high concentration periods) is generated by a TEI 49C-PS transportable primary standard ozone generator (S/N 0503110396) calibrated at ERLAP (European Reference Laboratory of Air Pollution) in May 2005 (initial calibration).

Aerosol

PM10 mass concentration: Tapered Element Oscillating Mass balance, Series 1400a

TEOM-FDMS S/N 140AB253620409 and S/N 8500B204110411

The Series 1400a TEOM® monitor incorporates an inertial balance patented by Rupprecht & Patashnick. It measures the mass collected on an exchangeable filter cartridge by monitoring the frequency changes of a tapered element. The sample flow passes through the filter, where particulate matter is collected, and then continues through the hollow tapered element on its way to an electronic flow control system and vacuum pump. As more mass collects on the exchangeable filter, the tube's natural frequency of oscillation decreases. A *direct* relationship exists between the tube's change in frequency and mass on the filter. The TEOM mass transducer does not require recalibration because it is designed and constructed from non-fatiguing materials. Calibration may be verified, however, using an optional Mass Calibration Verification Kit that contains a filter of known mass.

Standard use of TEOM® warms the sample at 40 or 50°C, in order to lower the air stream relative humidity. This temperature has a great influence on the volatilisation of particulate compounds with a low vapor pressure (negative artifacts), providing an underestimation of the PM mass.

To reduce this artifact, the instrument set-up can include a Sampling Equilibration System (SES) that allows a water strip-out without sample warm up by means of Nafion Dryers. In this way the air flow RH is reduced to < 30%, when TEOM® operates at 30°C only. A further development, the Filter Dynamic Measurement System (FDMS) is based on measuring changes of the TEOM filter mass when sampling alternatively ambient and filtered air. The changes in the TEOM filter mass while sampling filtered air is attributed to sampling (positive or negative) artifacts, and is used to correct changes in the TEOM filter mass observed while sampling ambient air.

The FDMS-TEOM was run at the JRC-Ispra station from March 14th to Nov. 12th, 2005, with a gap from Sept. 20th to Oct. 13th (Fig. 3).

Particle number size distribution: Differential Mobility Particle Sizer (DMPS)

DMA "A", CPC TSI 3760A S/N 141

The Differential Mobility Particle Sizer consists in a home-made medium size (28 cm) Vienna-type Differential Mobility Analyser (DMA) and a Condensation Particle Counter (CPC) TSI3760A.

DMAs use the fact that electrically charged particles move in an electric field according to their electrical mobility. Electrical mobility depends mainly on particle size and electrical charge. Atmospheric particles are brought in the bipolar charge equilibrium in the bipolar diffusion charger (TSI neutralizer): a radioactive source (Kr-85) ionizes the surrounding atmosphere into positive and negative ions. Particles carrying a high charge can discharge by capturing ions of opposite polarity. After a very short time, particles reach a charge equilibrium such that the aerosol carries the bipolar Fuchs-Boltzman charge distribution. A computer program sets stepwise the voltage between the 2 DMA's electrodes (from 10 to 11500V). Negatively charged particles are so selected according to

their mobility. After a certain waiting time, the CPC measures the number concentration for each mobility bin. The result is a particle mobility distribution. The number size distribution is calculated from the mobility distribution by an inversion routine (from A. Wiedensohler) based on the bipolar charge distribution and the size dependent DMA transfer function. The CPC detection efficiency curve is not taken into account. The DMPS measures aerosol particles in the range 6 - 500 nm and displays data using 54 size channels (32 channels per decade) for high-resolution size information. This submicrometer particle sizer is capable of measuring concentrations in the range from 1 to 2.4 x 10^6 particles/cm3. The DMPS generates a new particle size distribution every eight minutes. It is possible to set ambient pressure and temperature, so there is no need for post-acquisition data correction.

Accessories include:
- FUG High voltage cassette power supplies Series HCN7E – 12500 Volts.
- Membrane pump KNF (sampling aerosol at 1 cm³/min)
- Vacuum pump (circulating dry sheath air (<20% RH), using Silicagel, at 8.3 cc/min)
- Magnehelic for sheath air flow quick visual check

Particle number size distribution: Aerodynamic Particle Sizer (APS TSI 3321)

S/N 1243

The APS 3321 is a time-of-flight spectrometer that measures the velocity of particles in an accelerating air flow through a nozzle.

Ambient air is sampled at 1L/min, sheath air (from the room) at 4 L/min. In the instrument, particles are confined to the centerline of an accelerating flow by sheath air. They then pass through two broadly focused laser beams, scattering light as they do so. Side-scattered light is collected by an elliptical mirror that focuses the collected light onto a solid-state photodetector, which converts the light pulses to electrical pulses. By electronically timing between the peaks of the pulses, the velocity can be calculated for each individual particle.

Velocity information is stored in 1024 time-of-flight bins. Using a polystyrene latex (PSL) sphere calibration, which is stored in non-volatile memory, the APS Model 3321 converts each time-of-flight measurement to an aerodynamic particle diameter. For convenience, this particle size is binned into 52 channels (on a logarithmic scale).

The particle range spanned by the APS is from 0.5 to 20 μm in both aerodynamic size and light-scattering signal. Particles are also detected in the 0.3 to 0.5 μm range using light-scattering alone, and are binned together in one channel. The APS is also capable of storing correlated light-scattering-signal. *dN/dLogDp* data are averaged over 10 min. Maintenance by TSI in Sept. 2005.

Particle scattering and back-scattering coefficient (Nephelometer TSI 3563)

S/N 1081

The integrating nephelometer is a high-sensitivity device capable of detecting the scattering properties of aerosol particles. The nephelometer detects by measuring the light scattered by the aerosol and then subtracting light scattered by the walls of the measurement chamber, light scattered by the gas, and electronic noise inherent in the detectors.

Ambient air is sampled at 20L/min from a whole air inlet (TSP). The three-color detection version of TSI nephelometer detects scattered light intensity at three wavelengths (450, 550, and 700 nm). Normally the scattered light is integrated over an angular range of 7–170° from the forward direction, but with the addition of the backscatter shutter feature to the Nephelometer, this range can be adjusted to either 7–170° or 90–170° to give total scatter and backscatter signals. A 75 Watt quartz-halogen white lamp, with a built-in elliptical reflector, provides illumination for the aerosol. The reflector focuses the light onto one end of an optical pipe where the light is carried into

the internal cavity of the instrument. The optical pipe is used to thermally isolate the lamp from the sensing volume. The output end of the optical light pipe is an opal glass diffuser that acts as a *quasi*-cosine (Lambertian) light source. Within the measuring volume, the first aperture on the detection side of the instrument limits the light integration to angles greater than 7°, measured from the horizontal at the opal glass. On the other side, a shadow plate limits the light to angles less than 170°. The measurement volume is defined by the intersection of this light with a viewing volume cone defined by the second and fourth aperture plates on the detection side of the instrument. The fourth aperture plate incorporates a lens to collimate the light scattered by aerosol particles so that it can be split into separate wavelengths. The nephelometer uses a reference chopper to calibrate scattered signals. The chopper makes a full rotation 23 times per second. The chopper consists of three separate areas labelled: signal, dark, and calibrate.

The signal section simply allows all light to pass through unaltered. The dark section is a very black background that blocks all light. This section provides a measurement of the photomultiplier tube (PMT) background noise. The third section is directly illuminated this section to provide a measure of lamp stability over time. To reduce the lamp intensity to a level that will not saturate the photomultiplier tubes, the calibrate section incorporates a neutral density filter that blocks approximately 99.9% of the incident light. To subtract the light scattered by the gas portion of the aerosol, a high-efficiency particulate air (HEPA) filter is switched periodically in line with the inlet. This allows compensation for changes in the background scattering of the nephelometer, and in gas composition that will affect Rayleigh scattering of air molecules with time. When the HEPA filter is not in line with the inlet, a small amount of filtered air leaks through the light trap to keep the apertures and light trap free of particles. A smaller HEPA filter allows a small amount of clean air to leak into the sensor end of the chamber between the lens and second aperture. This keeps the lens clean and confines the aerosol light scatter to the measurement volume only.

The nephelometer lamp was replaced on June 20th, 2005, and annual maintenance performed by TSI in Sept-Oct. 2005.

Nephelometer data are corrected for angular non idealities and truncation errors according to Anderson and Ogren, 1998. Large hygroscopic effects are expected for internal RH > 60%, which can statistically occur from May to Sept. The nephelometer RH was recorded from June 25th, 2005, and inferred from met data for the reminder of the year. Atmospheric particle scattering coefficients presented in this report are **not** corrected for RH effects, except when specified.

Particle absorption coefficient (Aethalometer Magee AE-31)

S/N 408: 0303

The principle of the Aethalometer is to measure the attenuation of a beam of light transmitted through a filter, while the filter is continuously collecting an aerosol sample. Suction is provided either by an internally-mounted pump. Attenuation measurements are made at successive regular intervals of a timebase period. The objectives of the Aethalometer hardware and software systems are as follows:

(a) to collect the aerosol sample with as few losses as possible on a suitable filter material;
(b) to measure the optical attenuation of the collected aerosol deposit as accurately as possible;
(c) to calculate the rate of increase of the equivalent black carbon (EBC) component of the aerosol deposit and to interpret this as an EBC concentration in the air stream;
(d) to display and record the data, and to perform necessary instrument control and diagnostic functions.

The optical attenuation of the aerosol deposit on the filter is measured by detecting the intensity of light transmitted through the spot on the filter. In the AE-31, light sources emitting at different wavelengths (370, 450, 571, 615, 660, 880 and 950 nm) are also installed in the source assembly. The light shines through the lucite aerosol inlet onto the

aerosol deposit spot on the filter. The filter rests on a stainless steel mesh grid, through which the pumping suction is applied. Light penetrating the diffuse mat of filter fibers can also pass through the spaces in the support mesh. This light is then detected by a photodiode placed directly underneath the filter support mesh. As the EBC content of the aerosol spot increases, the amount of light detected by the photodiode will diminish.

For highest accuracy, we must make further measurements: the amount of light penetrating the combination of filter and support mesh is relatively small, and a correction is needed for the 'dark response signal' of the overall system. This is the electronics' output when the lamps are off: typically, it may be a fraction of a percent of the response when the lamps are on. To eliminate the effect of the dark response, we take 'zero' readings of the system response with the lamps turned off, and subtract this 'zero' level from the response when the lamps are on.

The other measurement necessary for the highest accuracy is a 'reference beam' measurement to correct for any small changes in the light intensity output of the source. This is achieved by a second photodiode placed under a different portion of the filter that is not collecting the aerosol, on the left-hand side where the fresh tape enters. This area is illuminated by the same lamps. If the light intensity output of the lamps changes slightly, the response of this detector is used to mathematically correct the 'sensing' signal. The reference signal is also corrected for dark response 'zero' as described above.

The algorithm in the computer program (see below) can account for changes in the lamp intensity output by always using the ratio quantity [Sensing]/[Reference]. As the filter deposit accumulates EBC, this ratio will diminish.

In practice, the algorithm can account for lamp intensity fluctuations to first order, but we find a residual effect when operating at the highest sensitivities. To minimize this effect and to realize the full potential of the instrument, it is desirable for the lamps' light output intensity to remain as constant as possible from one cycle to the next, even though the lamps are turned on and off again. The computer program monitors the repeatability of the reference signal, and issues a warning message if the fluctuations are considered unacceptable. When operating properly, the system can achieve a reference beam repeatability of better than 1 part in 10000 from one cycle to the next. The electronics circuit board converts the optical signals directly from small photocurrents into digital data, and passes it to the computer for calculation. A mass flow meter monitors the sampled air flow rate. These data and the result of the EBC calculation are written to disk and displayed on the front panel of the instrument.

Aethalometer data are corrected for the shadowing effect and for multiple-scattering in the filter to derive the aerosol absorption coefficient (Arnott et al., 2005) with a correction factor C = 3.65 for green light.

Sampling and off-line analyses

Particulate Matter

PM10 and PM2.5 from quartz fiber filters

$PM_{2.5}$ was continuously sampled at 16.7L/min on quartz fiber filters with a Partisol sampler, without charcoal stripe denuder and a $PM_{2.5}$ sampling head till July 31st, and with a dichotomous Partisol sampler without denuder from July 1st, 2005. The sampled area is 42 mm Ø in both samplers. Filters were from Schleicher & Schuell from January to November and from Whatman (QMA) for December.

PM_{10} was also collected with a Partisol automatic sampler, but with a charcoal parallel stripe denuder at 16.7 L/min (1 m³/hr) until July 31st. From July 1st, PMcoarse was collected with the dichotomous Partisol sampler, together with $PM_{2.5}$. Filter changes occurred daily at 08:00 UTC.

Filters were weighted before exposure at 50% RH and also 20% RH from November 2005. Filters were weighed at 50% (EN 12341 procedure) and 20% RH after exposure with a microbalance Sartorius MC5 placed in a controlled (dried or moisture added and scrubbed) atmosphere glove box. They were stored at 4°C until analysis.

Main ions (Cl$^-$, NO$_3^-$, SO$_4^{2-}$, C$_2$O$_4^{2-}$, Na$^+$, NH$_4^+$, K$^+$, Mg^{2+}, Ca^{2+}) were analysed by ion chromatography (Dionex DX 120 with electrochemical eluent suppression) after extraction of the soluble species in an aliquot of 16 mm Ø in 20 ml 18.2 MOhm cm resistivity water (Millipore mQ).

Organic and elemental carbon (OC + EC) were analyzed in PM10 and PM2.5 samples collected from January to April 2005 with a thermo-oxidative method (RA 10M) according to the following temperature and carrier gas change steps:

Fraction Name RA10M	Plateau Temperature (°C)	Carrier Gas
OC1.1	120	He:O$_2$ 80:20
OC1.2	220	He:O$_2$ 80:20
OC1.3	330	He:O$_2$ 80:20
OC2.1	450	He 100%
OC2.2	650	He 100%
EC1	650	He:O$_2$ 80:20
EC2	750	He:O$_2$ 80:20

PM10 samples collected from May to December 2005 and PM2.5 collected along the whole year 2005 were also analyzed for OC and EC using a Sunset Dual-optical Lab Thermal/Optical Carbon Aerosol Analyser (S/N 173-5) using a thermal program based on the Improve method and modified as follows:

Fraction Name Sunset Lab.	Plateau Temperature (°C)	Duration (s)	Carrier Gas
OC 1	200	120	He 100%
OC 2	300	150	He 100%
OC 3	450	180	He 100%
OC4	650	180	He 100%
OCPyr + EC1	550	240	He:O$_2$ 80:20
EC2	650	150	He:O$_2$ 80:20

OC$_{Pyr}$ and EC1 were split using the laser transmittance correction.

The OC4 temperature plateau was actually set to 550°C for analyzing samples collected from May to December 2005. The effect of OC4 the temperature set point on TC/EC will be determined *a posteriori*.

The comparison between total carbon (TC) and elemental carbon (EC) data measured in PM$_{2.5}$ over Jan.-Apr. 2005 with the two instruments (Fig. 5) shows that TC data are well correlated, and on average 12% smaller from the RA10M compared to the Sunset Lab. Instrument. In contrast, EC data are on average almost equal, but much more spread around the 1:1 line (R² = 0.61).
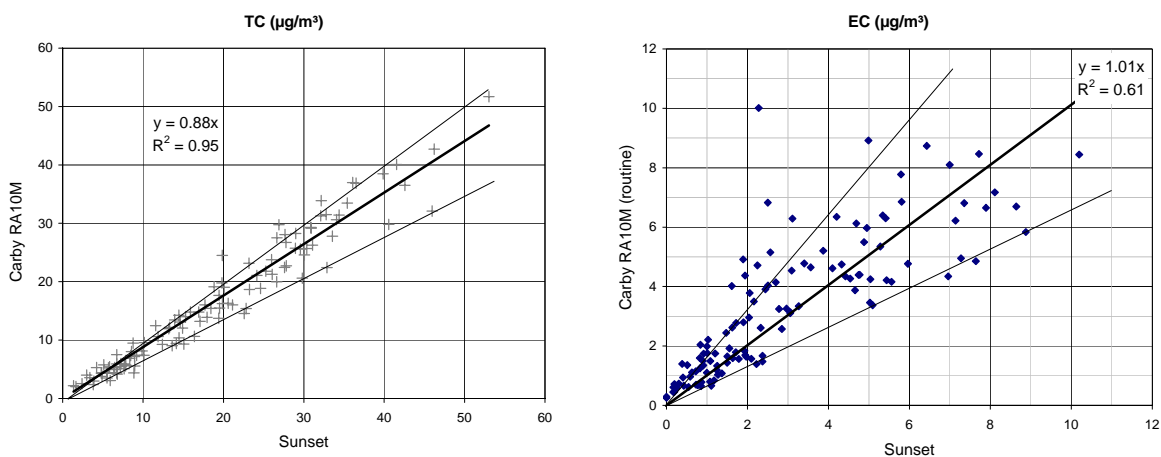

Fig. 5: comparison between the RA10M and the Sunset instruments for total carbon (TC) and elemental carbon (EC) determination.

Cellulose Whatman40 filters were also collected from April to September 2005.

Wet-only deposition

The AG *Elettronica Industriale* wet-only collectors are automatically opened and closed by a rain sensor and sample precipitations in a 10 l polythene container with a collection surface of about 660 cm^2. 24-hr integrated precipitation samples (if any) are collected every day at 10:00 UTC for week days, and on Monday morning for samples collected from Fri. 10:00 to Mon. 10:00.

All collected precipitation samples were stored at 4°C until analyses (ca.every 3 months). Analyses include the determinations of pH and conductivity at 25°C with a Sartorius Professional Meter PP-50 (from a single aliquot till April 2005 included, from 2 different aliquots onwards) and principal ion concentrations (Cl$^-$, NO$_3^-$, SO$_4^{2-}$, C$_2$O$_4^{2-}$, Na$^+$, NH$_4^+$, K$^+$, Mg^{2+}, Ca^{2+}) by ion chromatography (Dionex DX 120 with electrochemical eluent suppression).

Quality assurance

At JRC level the quality system is based on the Total Quality Management philosophy, the implementation of which started at the Environment Institute in December 1999. Lacking personnel to specifically follow this business, the JRC-Ispra air monitoring station did not renew the accreditation for the monitoring of SO_2, NO, NO_2 and O_3 under EN 45001 obtained in 1999. However, most measurements and standardized operating procedures are based on recommendations of the EMEP manual (1996), WMO/GAW, ISO and CEN standards. Moreover, the JRC-Ispra gas monitors and standards are checked by the European Reference Laboratory for Air Pollution (ERLAP) regularly (see specific measurement description for details). In contrast, no framework for audit and intercalibration of on-line aerosol instrument was in place in 2005. Most instruments were regularly calibrated through maintenance contracts though.

The analytical laboratory of the JRC-Ispra station takes regularly part in international intercomparison exercises. The yearly EMEP intercomparison for rainwater analyses (Fig. 6) shows enhanced discrepancies relative to the average (up to 35%) for the last years (from 1999).Brand new IC standards were purchased and used for IC calibration from 2006

Data quality is also checked whenever possible through comparison among different instruments (for gases), mass closure (for PM) and ion balance (for precipitation) exercises.
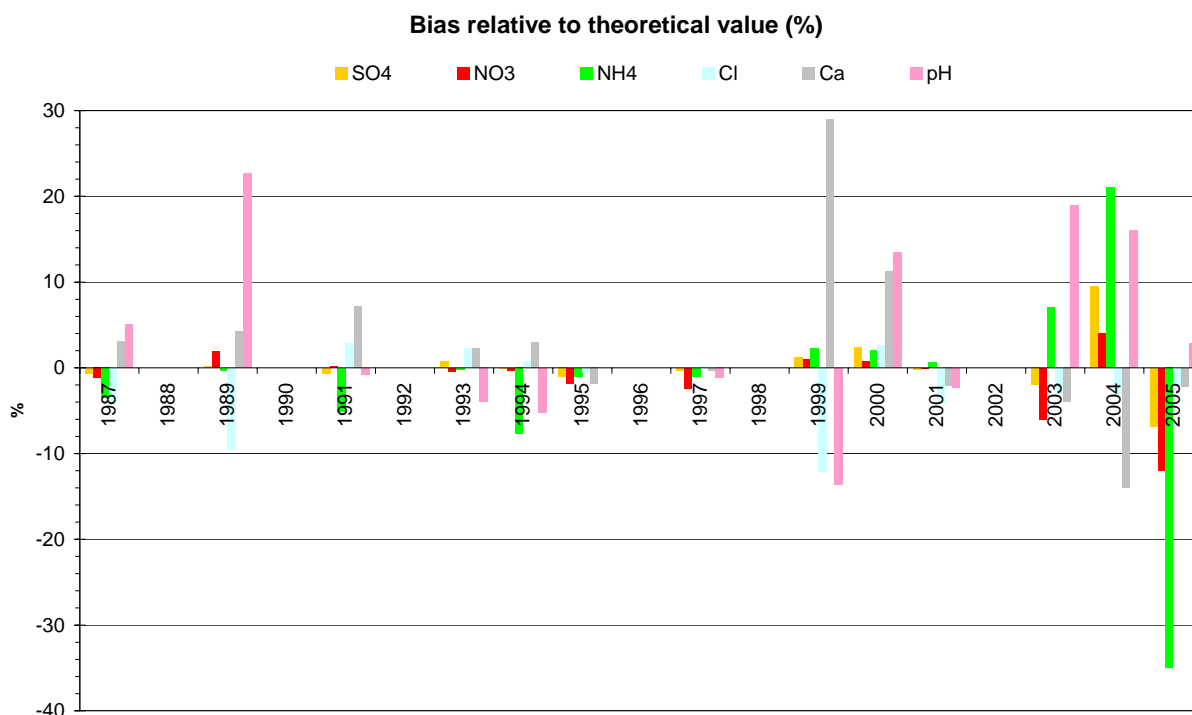
Fig. 6: JRC-Ispra results of the EMEP intercomparisons for rainwater analyses
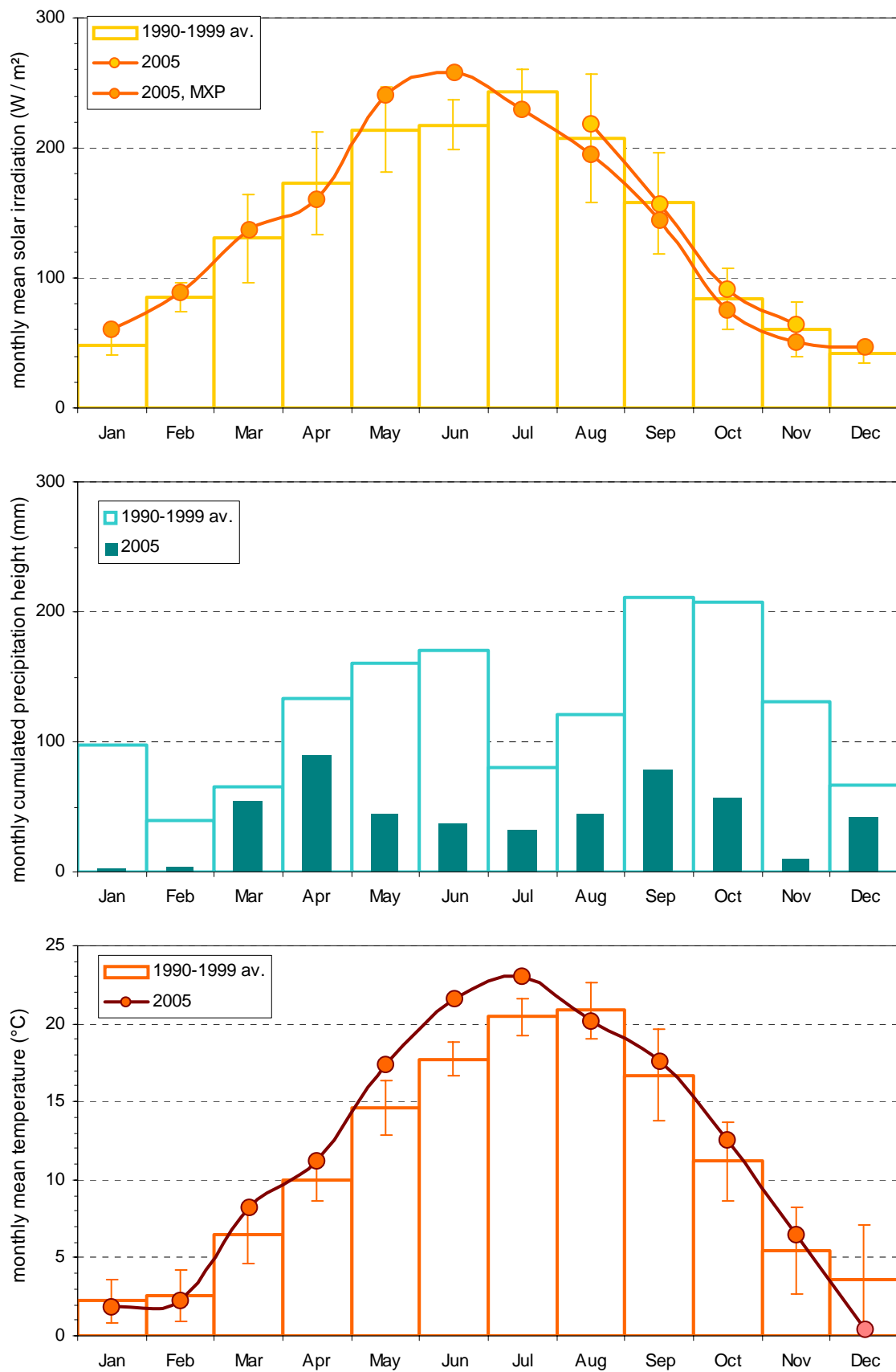
Fig. 7: solar global irradiation, precipitation amount, and temperature monthly means observed at JRC-Ispra(and Malpensa airport, MXP) in 2005, compared to the 1990-1999 period ± standard deviation.

Results of the year 2005.

Meteorology

Meteorological data for 2005 were obtained from sensors located at Bd 51 (about 1.5 km SW of the station), and also from Malpensa (MXP) airport (solar irradiation).

Fig. 7 shows monthly values of meteorological parameters for 2005 compared to the 1990-1999 average.

It can be noticed that solar irradiation data from MXP are systematically lower (ca. -15%) than the ones obtained in Ispra. Therefore, solar irradiation monthly means were comparable with the 1990-1999 average, except for May and June, which were significantly more sunny than usual.

Precipitation amount was lower than usual (1990-1999 average) over the whole year. The annual precipitation amount (831 mm) was the lowest ever recorded at the station since 1986, equal to 60% of the usual (1990-1999 average) annual rainfall and ca. 20% lower than the previous (2003) record.

Also temperature was higher than usual (1990-1999 average) in May – July 2005, but quite low in December.
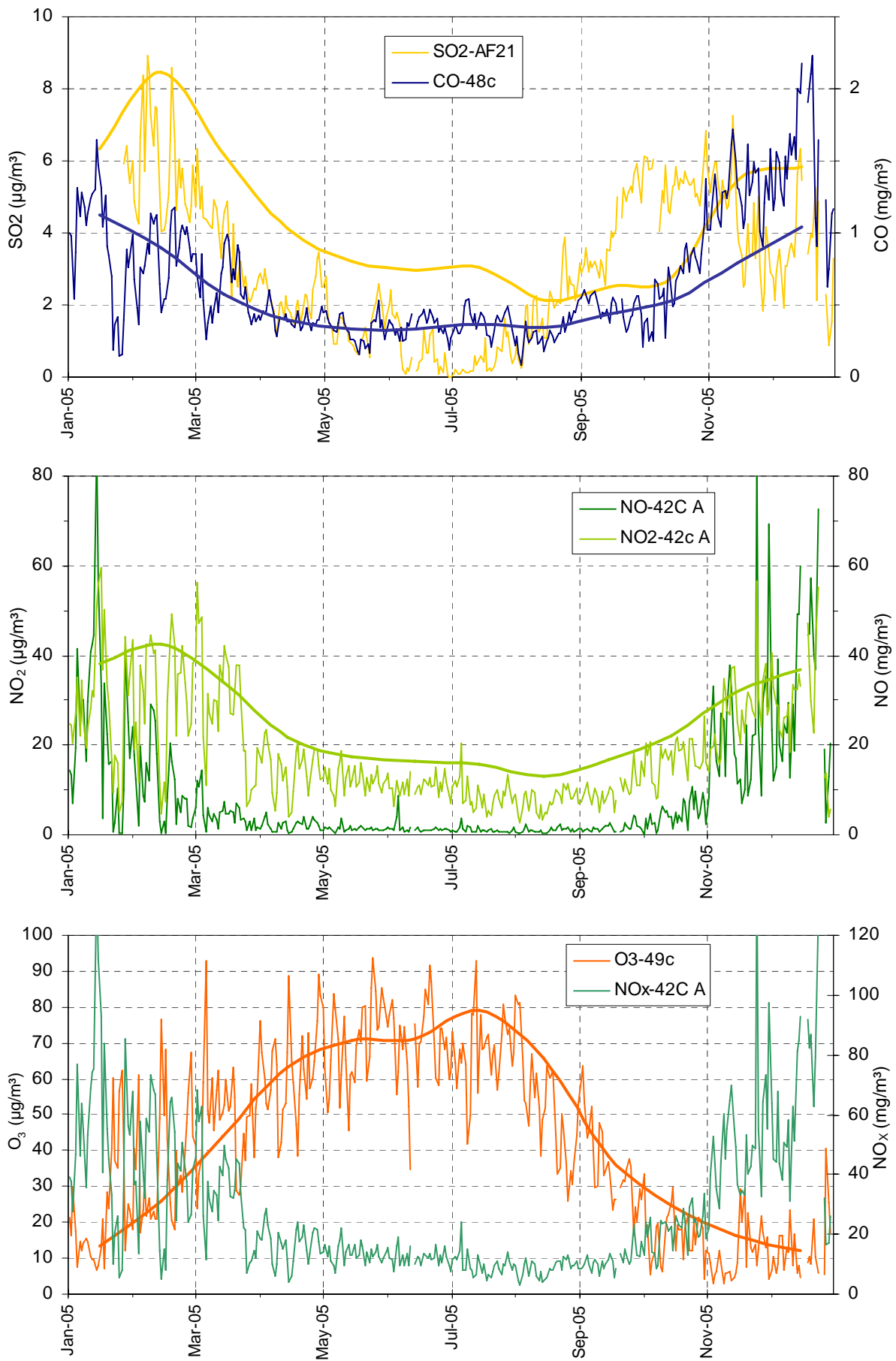
Fig. 8: *Variations in 24 hr averaged concentrations of SO₂, CO, NO₂, NO, O₃ and NOx in 2005 (thin lines) and 1990-1999 averages (thick lines).*

Gas phase

Gas phase measurements were carried out over the whole year 2005, starting from Jan. 27th for SO$_2$. Seasonal variations in SO$_2$, CO, NO, NO$_2$, NOx and O$_3$ were comparable to those observed over the 1990-1999 period (Fig. 8), with higher concentrations during wintertime for primary pollutants, and higher concentrations in summer for O$_3$, resulting from photochemical atmospheric reactions.

Concentrations of CO were generally in line with the 1990-1999 average (Fig. 8), except for the 21-28 Jan. period, when they were lower, due to unusual meteorological conditions (strong wind, several days with Foehn). In contrast, CO concentrations were a little larger than usual from Nov. to mid-Dec. SO$_2$ concentrations were lower than usual except in Sep.- Oct. 2005. Specially low SO$_2$ concentrations were observed in Nov.- Dec. 2005, which can be partially explained by frequent precipitations during late Nov.- early Dec. NO$_2$ concentrations were generally lower than observed over 1990-1999, but did not show any further decrease compared to 2004.

Also O$_3$ concentrations were slightly lower in 2005 compared to 1990-1999. The high O$_3$ levels observed over several days from January to March 2005 were all associated with high wind speed and low relative humidity, which characterize Foehn events and might lead to the transport of high altitude O$_3$ to the ground. The vegetation exposure to above the ozone threshold of 40 ppb (AOT 40) amounted 16880 ppb h (with a data coverage for O$_3$ of 95%), to be compared to 34000 ppb h / yr over the 1990-1999 decade (Fig. 9). Over Apr. – Sep. (O$_3$ data coverage = 96 %), AOT40 (15350 ppb h) was also twice smaller than over the 1990-1999 period (32000 ppb h). SOMO35 (population exposure to above 35 ppb O$_3$) was 2680 ppb day. **For the fist time since 1987, the O$_3$ population information warning level** (180 µg/m³) **was never reached in 2005**, to be compared with 29 exceedances / yr on average over the 1990-1999 decade.
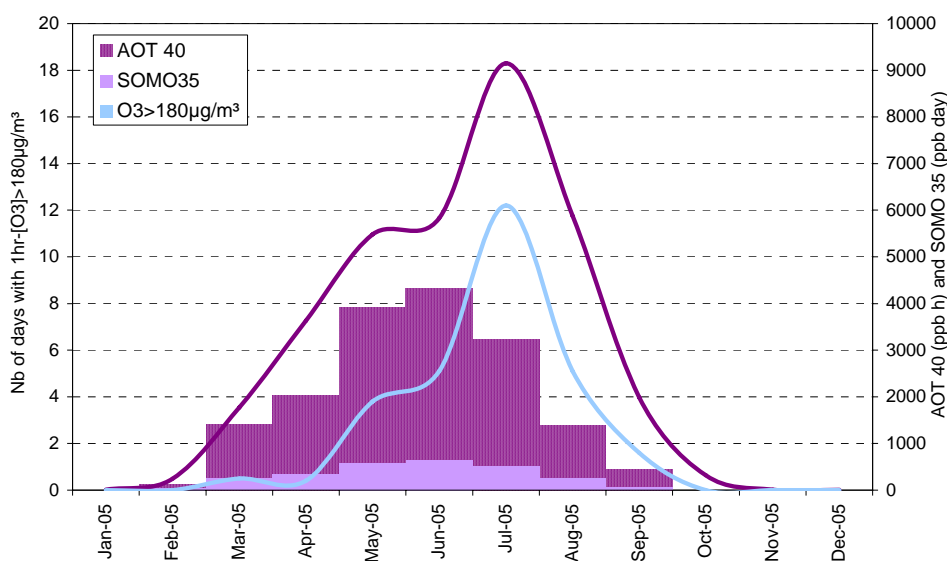

Fig. 9: AOT 40 and SOMO values in 2005 (bars), and AOT 40 and number of exceedances of the 1-hr averaged 180 µg/m³threshold over 1990-1999 (lines) No exceedance was observed in 2005 .
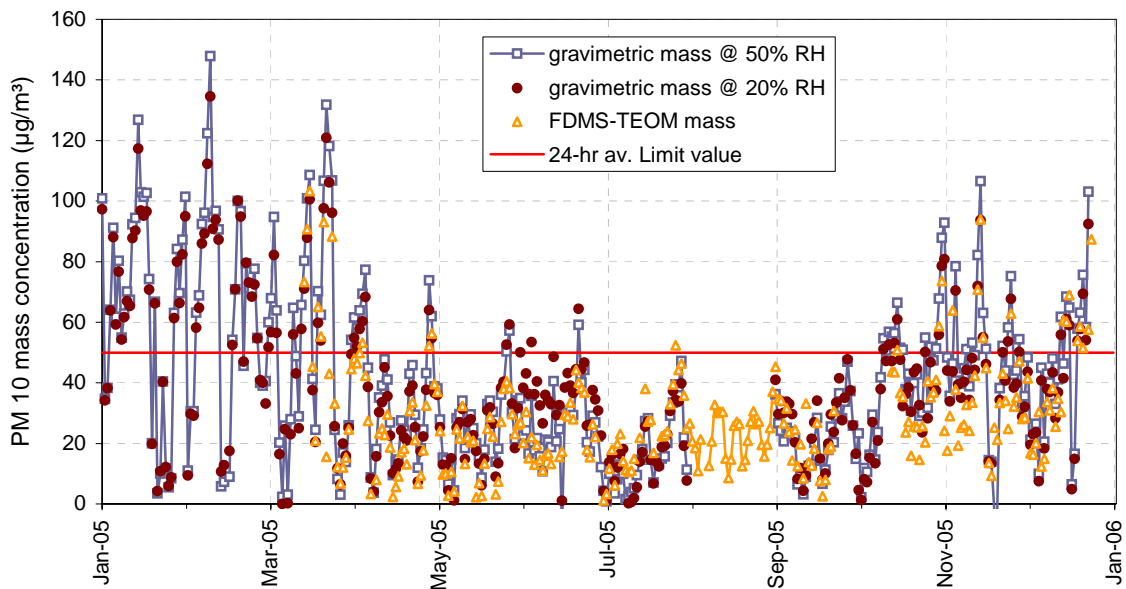
Fig. 10: 24 hr-integrated PM10 from off-line gravimetric measurements at 50% and 20% RH, and 24-hr averaged on-line FDMS-TEOM PM10 mass concentrations in 2005. The red line shows the 50 µg/m³ 24-hr limit value.
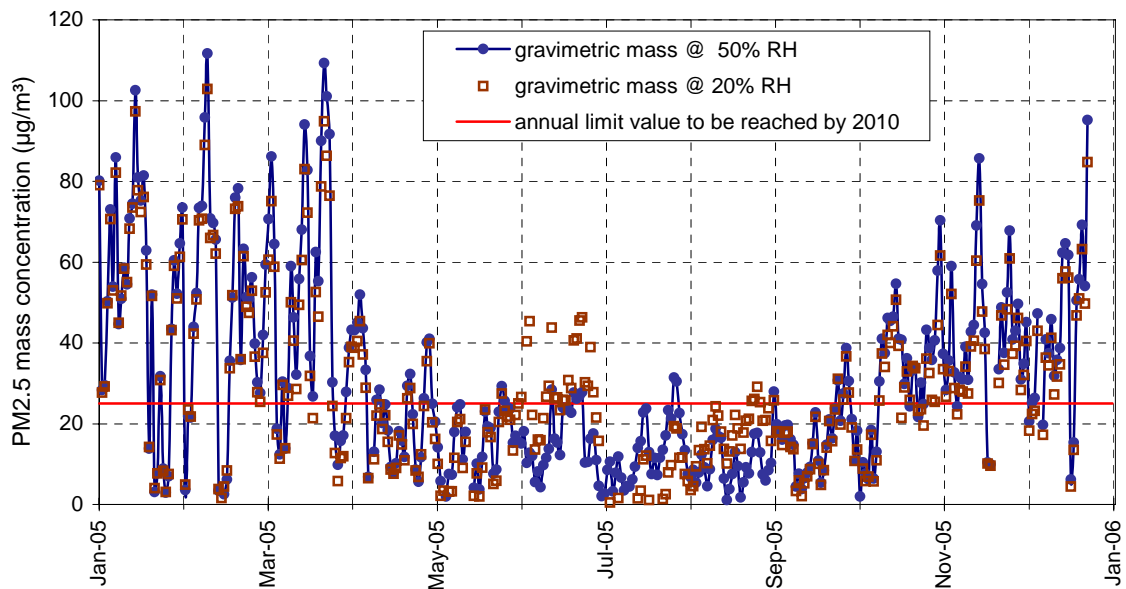

Fig. 11: 24hr-PM2.5 mass concentrations from off-line gravimetric measurements at 50 and 20% RH in 2005.
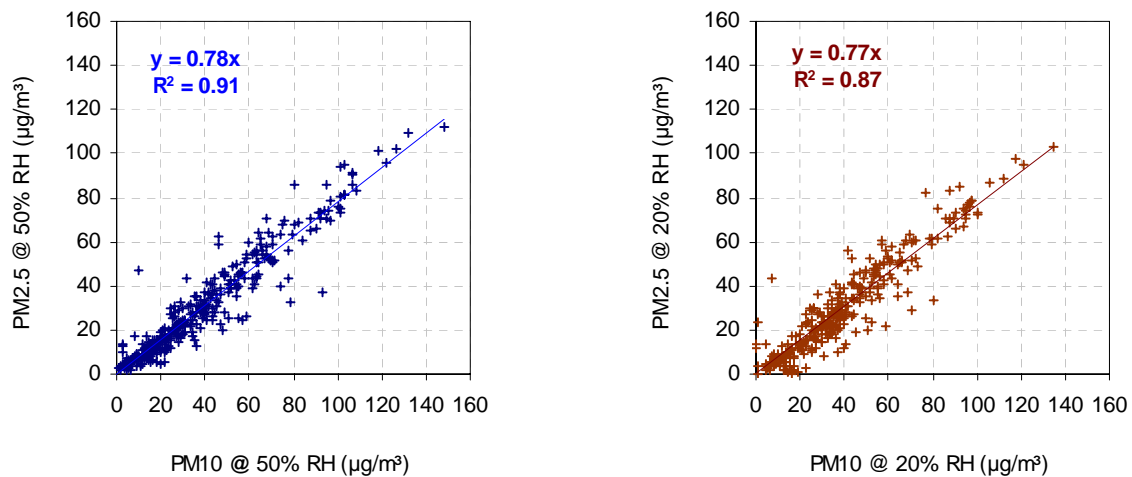

Fig. 12: correlation between PM10 and PM2.5 mass concentrations measured at 50% and 20% RH over 2005

Particulate phase

Particulate matter mass concentrations

PM10 annual mean concentration over 2005 was 41.2 µg/m³, i.e. above to the European annual limit value (40 µg/m³). The PM10 24-hr EU limit value (50 µg/m³) was exceeded 99 times (Fig. 10), whereas the European directive **1999/30/EC** states that it should not to be exceeded more than 35 times a calendar year from 2005. PM2.5 annual mean concentration (Fig. 11) was 29.8 µg/m³ (1.5 µg/m³ larger than in 2004), i.e. well above the envisaged European annual limit value (25 µg/m³) to be reached by 2010. PM2.5 and PM10 concentrations were well correlated at both 50 and 20% RH, with PM2.5 / PM10 ratios (slopes) equal to 0.78 and 0.77, respectively, i.e. not significantly different from the previous years (Fig. 12). Regressions between gravimetric measurements carried out at 20 and 50% RH show that PM10 weighing at 20% RH consistently lead to lower values than weighing at 50% (Fig. 13), suggesting that 7-9 % of PM2.5 and PM10 measured at 50% RH consist of water.
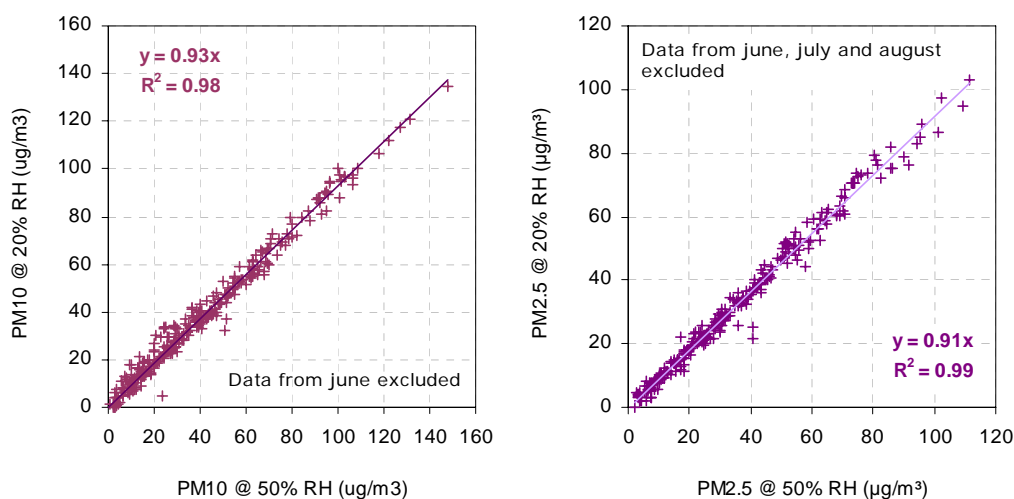
Fig. 13: regressions between gravimetric measurements at 20 and 50% RH ,for (a) PM10 and (b) PM2.5

On-line PM10 mass measurements were performed with the FDMS-TEOM from March 14th to Nov. 12th, 2005. Over this period, the 24-hr av. concentrations derived from the FDMS-TEOM measurements were generally lower than the gravimetric measurements operated at both 50% and 20% RH (Fig. 14), in contrast with what was observed over previous years.
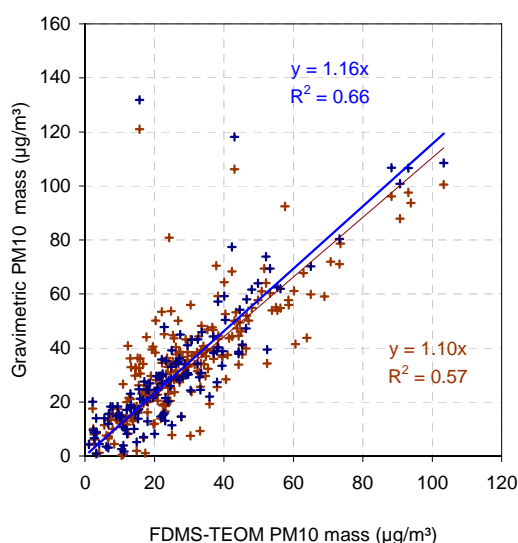

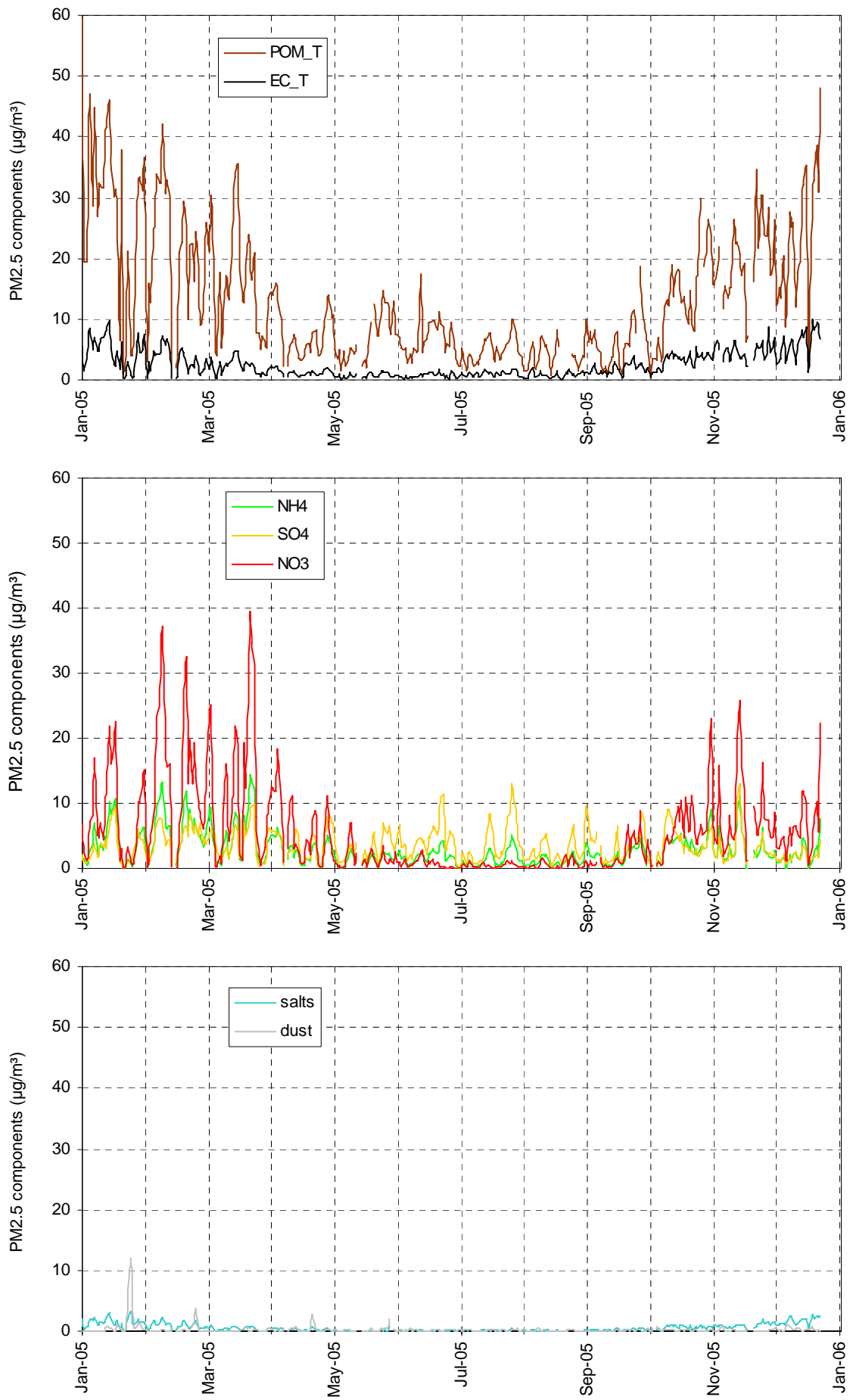*Fig. 14: regressions between FDMS-TEOM and gravimetric PM10 values at 20 (red) and 50% (blue) RH.*

Fig. 15: 24-hr integrated concentrations of the main aerosol components in PM2.5 over 2005

PM2.5 chemistry

Main ions (Cl^-, NO_3^-, SO_4^{2-}, $C_2O_4^{2-}$, Na^+, NH_4^+, K^+, Mg^{2+}, and Ca^{2+}), OC and EC were determined from the quartz fiber filters collected for PM mass concentration measurements, as usual. Fig. 15 shows the variations in the PM2.5 main components derived from these measurements. Particulate organic matter (POM) is calculated by multiplying OC values by the 1.4 conversion factor to account for non-C atoms contained in POM. "Salts" include Na^+, K^+, Mg^{2+}, and Ca^{2+}. Dust is calculated from Ca^{2+} concentrations and the slope of the regression found between ash and Ca^{2+} in the analyses of ashless cellulose filters (Whatman 40) in previous years (4.5). Most components show seasonal variations with higher concentrations in winter and fall, and lower concentrations in summer, like PM2.5 mass concentrations. This is mainly due to changes in pollutant horizontal and vertical dispersion, related to seasonal variations in meteorology. The amplitude of the POM and NO_3^- seasonal cycles may be enhanced due to equilibrium shifts towards the gas phase, and/or to enhanced losses (negative artifact) from quartz fiber filters during warmer month. SO_4^{2-} concentrations larger than 10 µg/m³ were observed in May and June 2005, which suggests that enhanced photochemical production of SO_4^{2-} during sunny days can compensate for the increased aerosol dilution due to convection.

NH_4^+ generally follows $NO_3^- + SO_4^{2-}$, as indicated by the regression shown in Fig. 15. This correlation results from the atmospheric reaction between NH_3 and the secondary pollutants H_2SO_4 and HNO_3 produced from SO_2 and NOx, respectively. Over 2005, the slope of this regression is close to 1, which means that NH_3 was sufficient to neutralise both H_2SO_4 and HNO_3. This indicates that PM2.5 aerosol was generally not acidic in 2005.
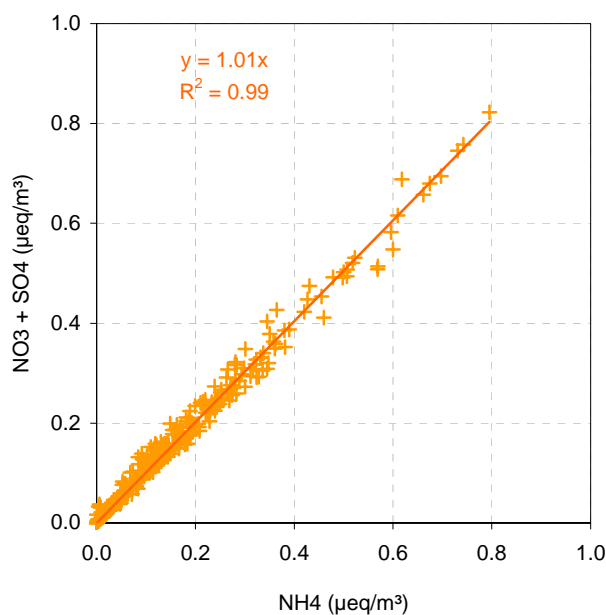

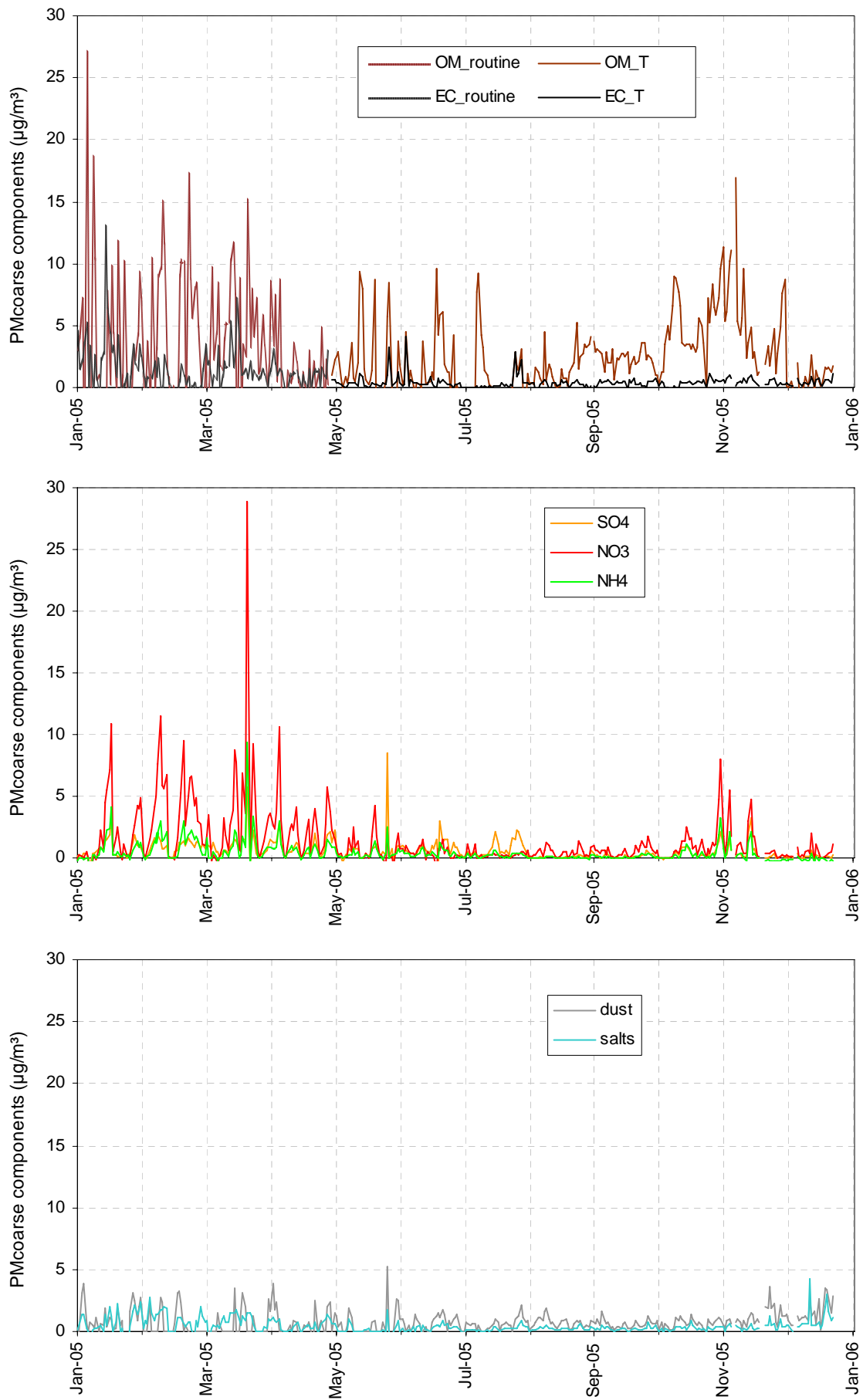*Fig.15: $SO_4^{2-} + NO_3^-$ vs. NH_4^+ (µeq/m³) in PM 2.5 over 2005.*

*Fig. 16: 24-hr integrated concentrations of the main aerosol components in **PMcoarse** over 2005*

PMcoarse chemistry

The same components as in $PM_{2.5}$ were measured in PM_{10} from Jan. to July, and in PMcoarse, as collected with the Partisol dichotomous sampler, from August to December. PMcoarse component concentrations were calculated as the difference between PM_{10} and $PM_{2.5}$ for Jan. July 2005. The seasonal variations in PMcoarse components are similar to the ones observed in $PM_{2.5}$, which much smaller concentrations though, except for "salts" and "dust", that are about equally distributed among the coarse and the fine ($PM_{2.5}$) aerosol fractions. Peaks in coarse NO_3^- and SO_4^{2-} were exceptionally observed in March and May 2005 (Fig. 16). As in PM2.5, POM is generally the main component of the aerosol coarse fraction. No clear Ca^{2+} peak denoting significant transport of Saharan dust out of rainy periods was observed over 2005.

NH_4^+ and SO_4^{2-} + NO_3^- (in µeq/m³) were well correlated over 2005, and the regression slope indicates that NH_4^+ was generally more than sufficient to neutralize both H_2SO_4 and HNO_3 acidities in the PMcoarse fraction (Fig. 17). NH_4^+ excess may be bound to not measured organic acids. There is no case where NO_3^- + SO_4^{2-} is larger than NH_4^+, which would suggest the association of NO_3^- and / or SO_4^{2-} to other counter-ions, like Na^+, Mg^{2+}, or Ca^{2+} for instance.
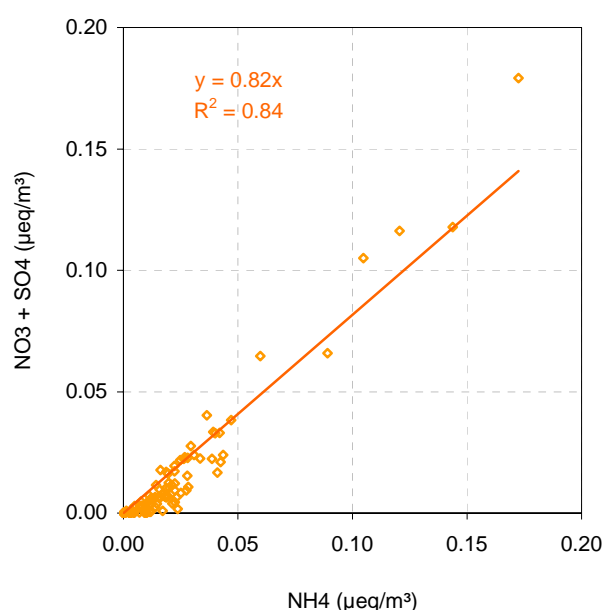

Fig 17: SO_4^{2-} + NO_3^- vs. NH_4^+ (µeq/m³) in PMcoarse over 2005.

PM10 chemistry

As PM2.5 accounted for close to 80% of PM10 mass concentration, most components of PM10 presented seasonal variations comparable to the ones observed in PM2.5, with higher concentrations in winter and fall, and lower concentrations from April to October, except for SO_4^{2-} which presents lower concentrations in winter compared to the rest of the year.
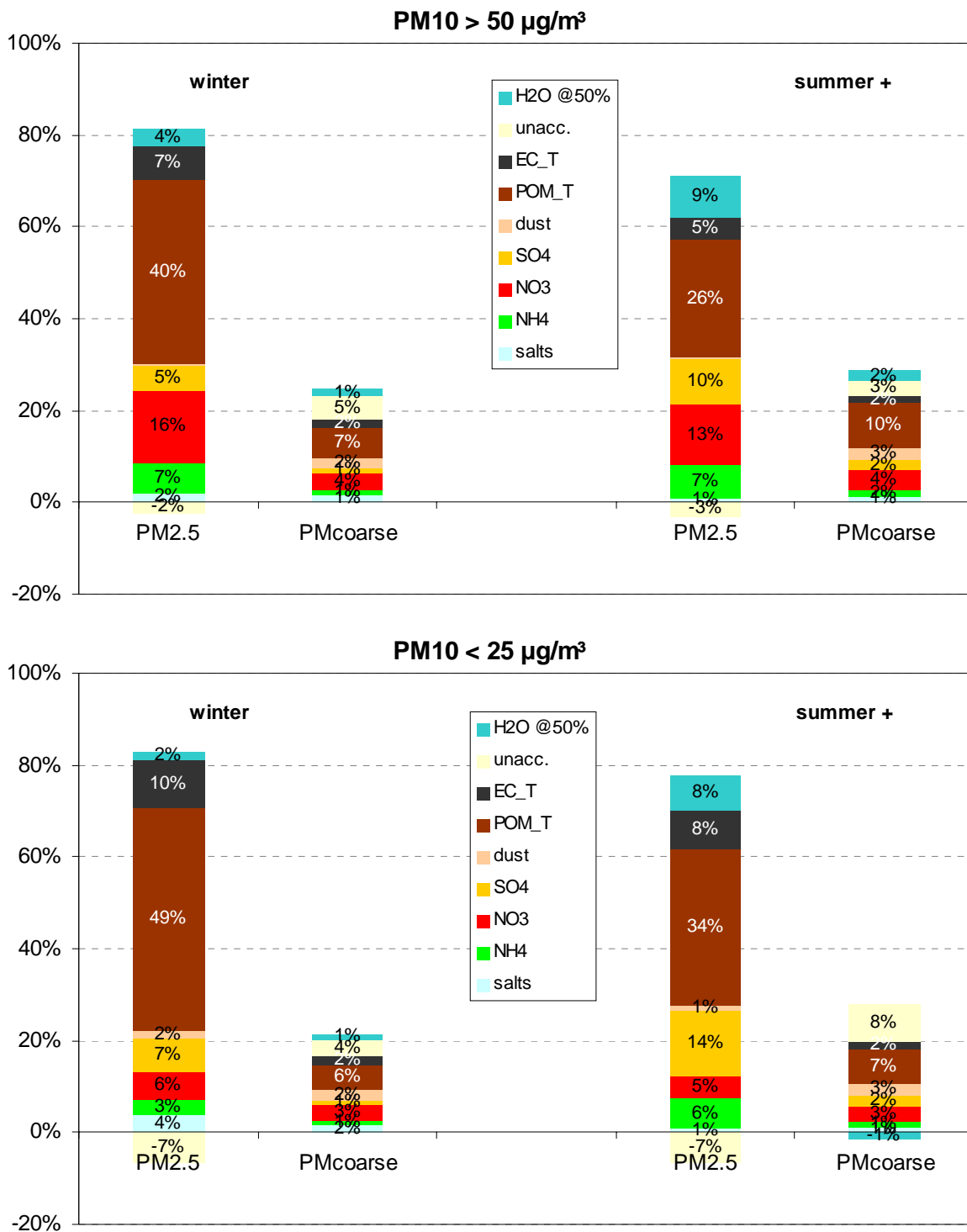
Fig. 18: average contribution of PM2.5 and PMcoarse components to PM10 mass concentration determined from gravimetric measurements at 50% RH, for days on which PM10 > 50µg/m³(top) and PM10 < 25 µg/m³(bottom), in winter (Jan., Feb., Dec.) and extended summer (Apr. – Oct.).

<u>Contribution of the main aerosol components to PM10 during high and low PM10 concentration periods observed in winter and (extended) summer</u>

The contributions of the main aerosol components to PM_{10} in each size class ($PM_{2.5}$ and PMcoarse) is presented (Fig. 18, top) for days on which the 24-hr limit value of 50 µg/m³ was exceeded, in winter (Jan., Feb. and Dec., 48 cases) and extended summer (Apr. to Oct, 9 cases).

No PM_{10} exceedances were observed in summer (Jun.-Aug). These PM_{10} compositions may not always represent accurately the actual composition of particulate matter in the atmosphere (due to various sampling artifacts), but are suitable to assess which components (in which fraction) contributed to the PM_{10} mass concentration when measured according to the normative rules described in EN12341 (i.e 50% RH).

During wintertime, the aerosol coarse fraction contributed to high PM_{10} concentrations (>50 µg/m³) for ca. 20 %.This is more than in 2003 (10%) and 2004 (15%). Dust, which is mainly found in the coarse fraction, represented only 2% of PM10. Carbonaceous species (POM and EC) represented a much larger fraction of PM_{10} (> 50%) than secondary inorganic species NH_4NO_3 and $(NH_4)_2SO_4$ (34%), and were mainly present in the fine fraction ($PM_{2.5}$). Water accounted for 5% on average of the PM mass (for $PM_{10} > 50$µg/m³).

During the extended summer season (Apr. to Oct.), the coarse fraction contributed for close to 30% to PM_{10} concentrations larger than 50 µg/m³. The coarse aerosol fraction was mainly made of carbonaceous species (POM + BC). The contribution of NO_3^- to the aerosol coarse fraction was as low as in 2003, probably because no large mineral dust transport occurred in 2005 (like in 2004), which would have shifted NO_3^- from the fine to the coarse aerosol mode (through reactions between dust and HNO_3) like in 2003. Altogether (coarse and fine), inorganic secondary species (NH_4NO_3 and $(NH_4)_2SO_4$) made up 38% of PM_{10} over days on which PM_{10} exceed 50 µg/m³ in Apr. – Oct. 2005, vs. 43% from carbonaceous species. Water accounted for 11% of PM_{10} mass measured at 50% RH, i.e. twice as much as in winter.

On cleaner days ($PM_{10} < 25$ µg/m³), the distribution of PM_{10} among $PM_{2.5}$ and PM_{coarse} does not change significantly compared to more polluted days ($PM_{10} > 50$ µg/m³). The contribution of carbonaceous components (POM and EC) reaches 56% in winter and 51% in summer, vs. 21% and 29% for secondary inorganic components, respectively. Specially the share of EC (12 % in winter, 10 % in summer) is larger than on cleaner days, which indicate a larger contribution of local sources, whereas secondary (regional) aerosol contribution is larger on more polluted days.
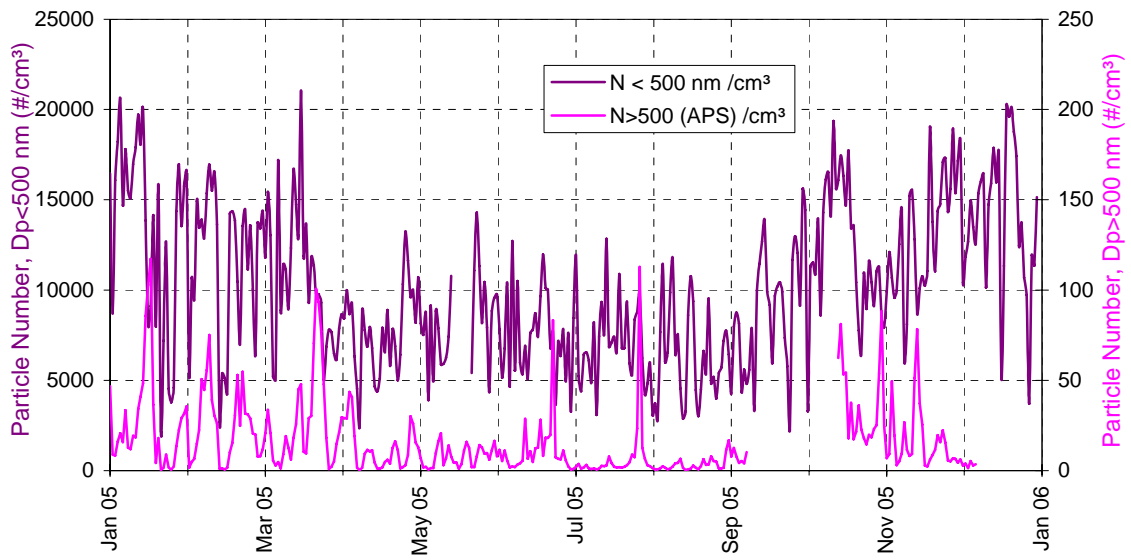
.

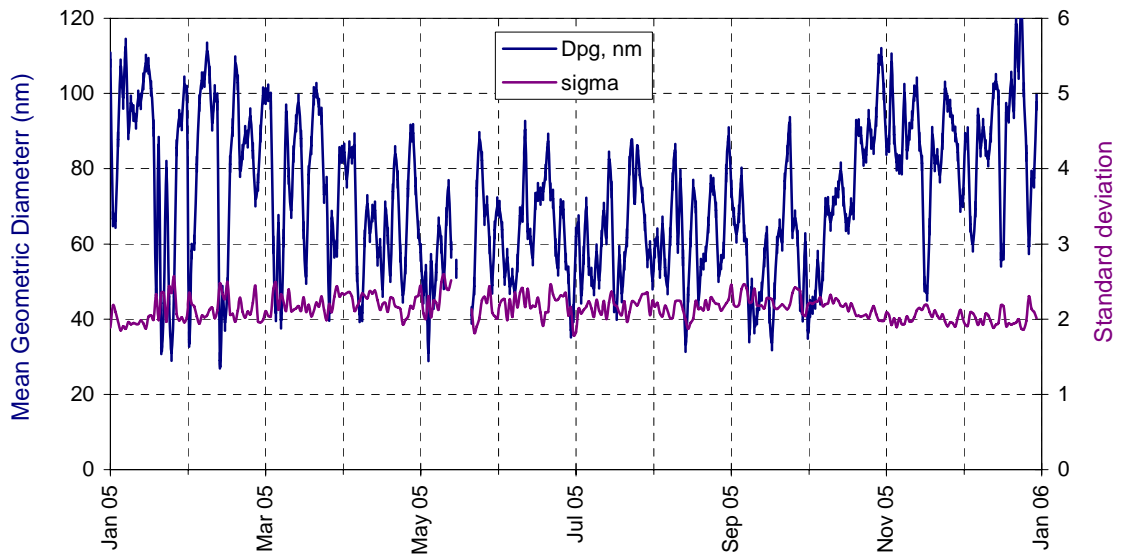*Fig. 19: 24 hr - averaged particle number concentrations for Dp>500 nm and Dp<500 nm*

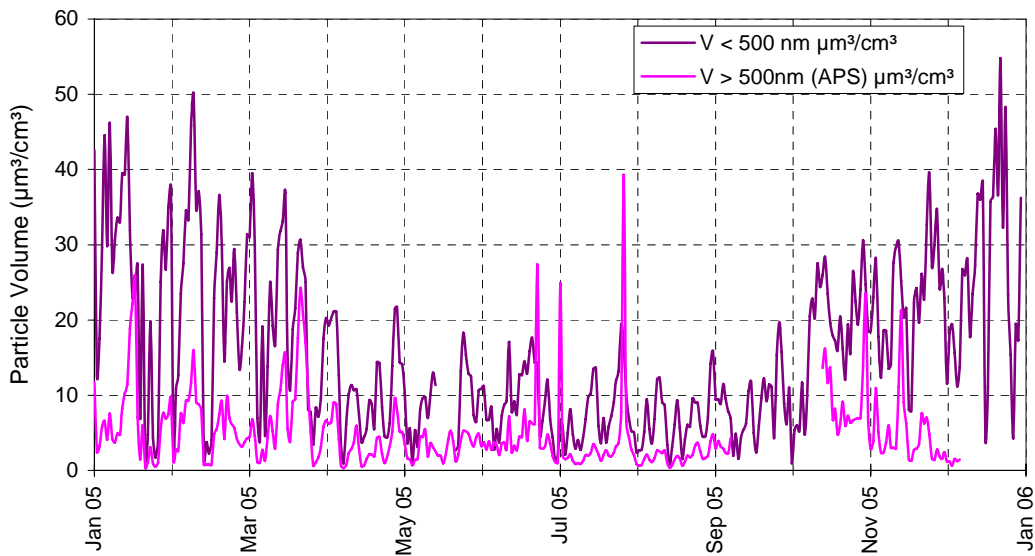*Fig. 20: 24 hr - averaged particle geometric mean diameter and standard deviation*

Fig. 21: 24 hr - averaged particle volume concentrations for Dp>500 nm and Dp<500 nm

Aerosol physical properties

Measurements of the particle number size distributions smaller than 500 nm diameter were carried out using a Differential Mobility Particle Sizer over the whole year 2005. Particle number concentrations averaged over 24 hr (from 08:00 to 08:00 UTC) ranged from 2100 to 21000 cm^{-3} (average: 10000 cm^{-3}) and followed a seasonal cycle comparable to that of PM mass concentration, with maxima in winter and minima in summer (Fig. 19).

The variations in particle number size distributions parameters at RH<20% (Fig. 20) show clear seasonal patterns: the mean geometric diameter is generally larger in winter than in summer, whereas the standard deviation of the distribution follows an opposite trend (larger in summer than in winter). The size distribution of particles larger than 500 nm was measured over most of the year using an Aerodynamic Particle Sizer (aerodynamic converted to geometric diameter using a particle density of 1.50). As previously observed, particles larger that 500 nm accounted on average for 0.2% of the total particle number only (Fig. 19), but for 36% of the total particle volume (Fig. 21). The seasonal variations in particle volume concentration reflect the changes in particle number and mean geometric diameter, with larger volumes in winter than in summer. Looking at particle number size distributions reveals a reasonable agreement among the APS and the DMPS across the 4 seasons of the year (Fig. 22).
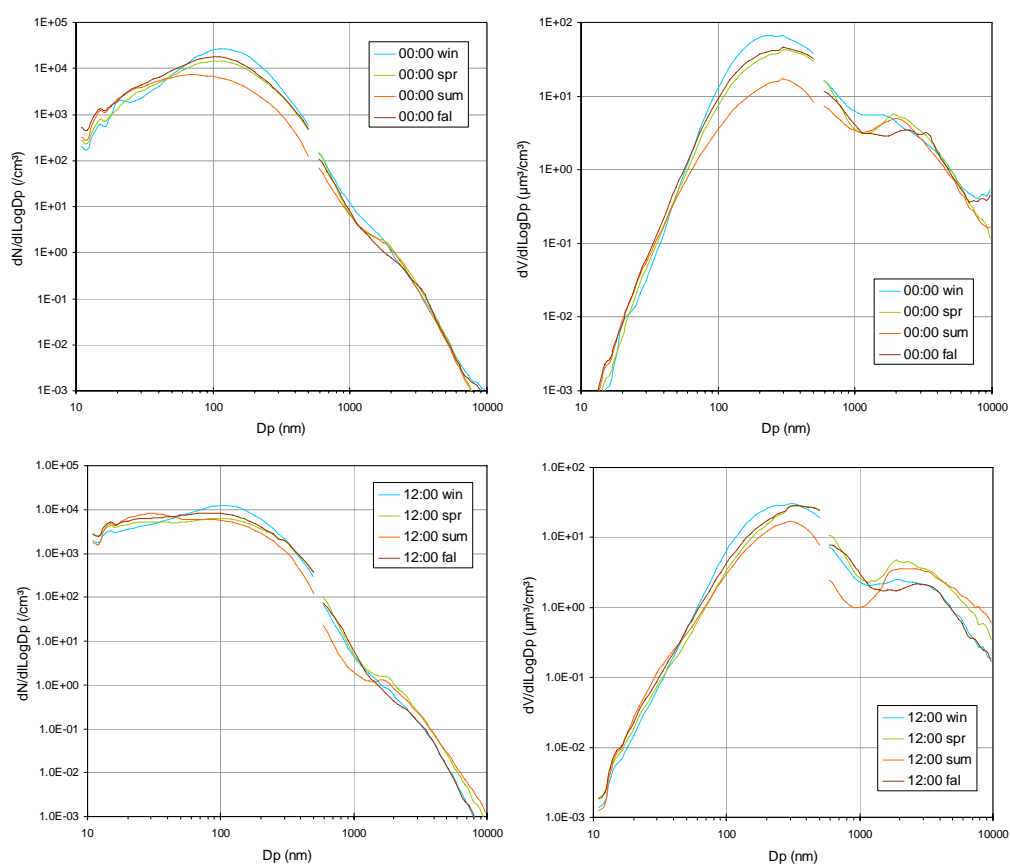

Fig. 22:seasonal mean particle number and volume size distributions at 00:00 and 12:00 UTC measured with a DMPS (10-500 nm) and an APS (0.65-10µm).
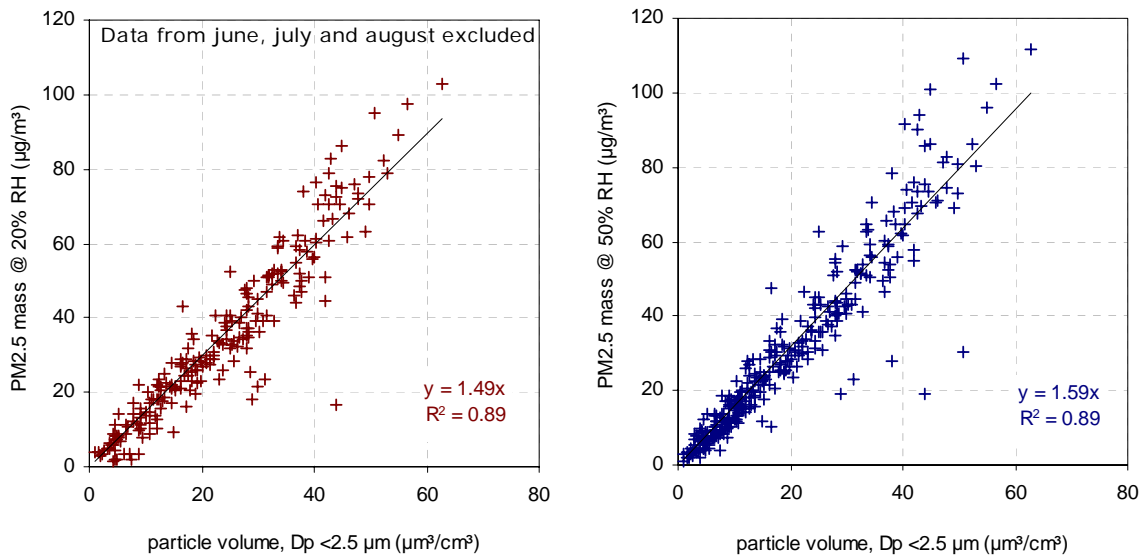
Fig. 23: regressions between PM$_{2.5}$ mass concentrations determined from gravimetric measurements at 20 and 50% RH and particle volume (Dp<2.5 μm) calculated from DMPS and APS measurements.
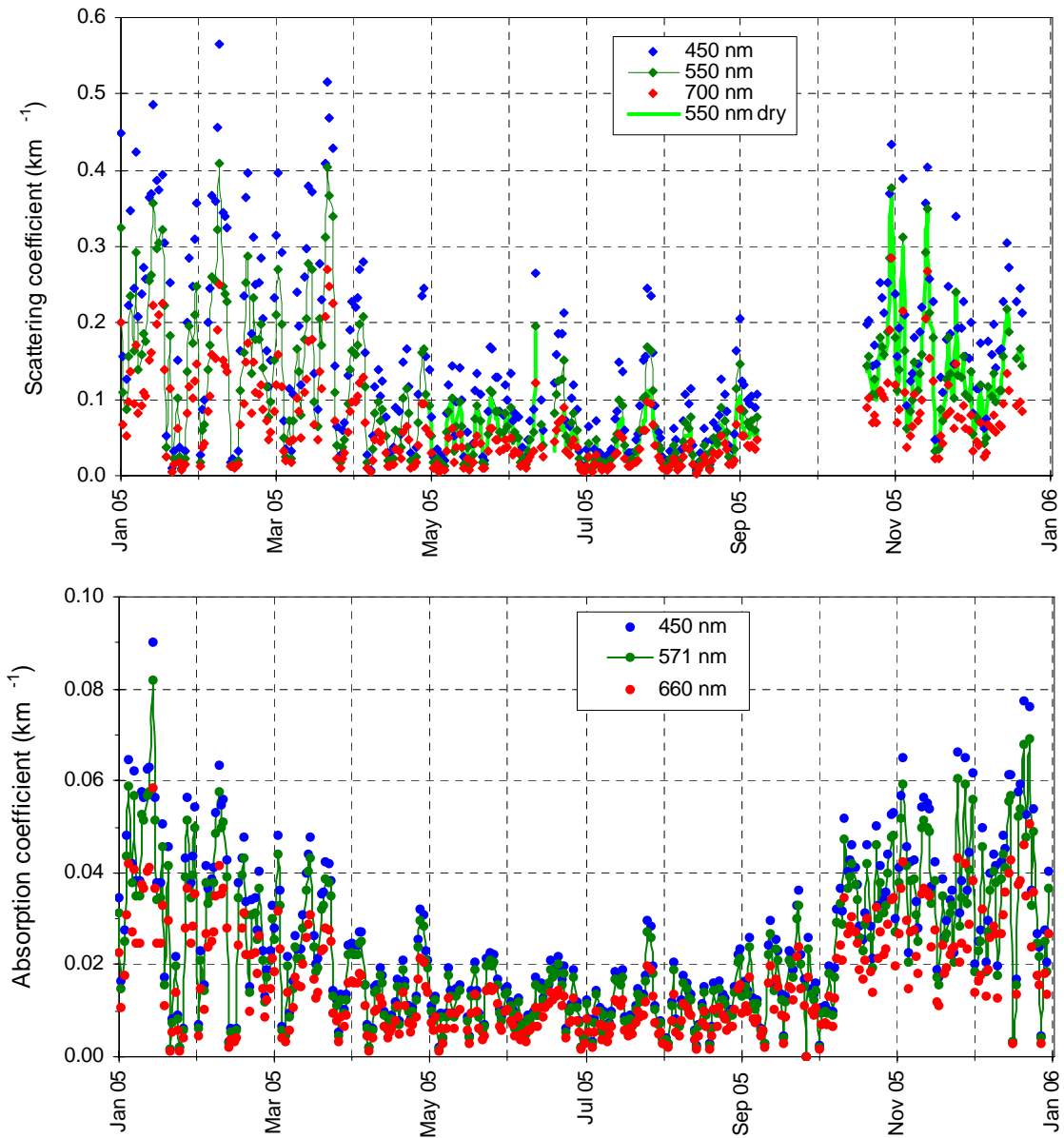

Fig. 24: daily mean atmospheric particle scattering and absorption coefficients at three wavelengths, derived from Nephelometer and Aethalometer measurements (not corrected for RH, except if specified).

The comparison between PM$_{2.5}$ mass and aerosol volume concentration (for aed < 2.5 µm) shows good correlations (Fig. 23). The slope of the regression between PM$_{2.5}$ at 20% RH and particle volume suggests an aerosol density close to 1.5, which is consistent with the density used to convert the aerodynamic diameter of the APS to geometric diameters. As PM$_{2.5}$ mass concentrations at 20% RH are not available for June, July and Aug. 2005, also the regression with PM$_{2.5}$ at 50% is presented, to show that the correlation coefficient does not decrease when data from the whole year are considered.

Aerosol optical properties

Aerosol optical properties have been monitored continuously over 2005, except for maintenance periods (Fig. 24). Data from the Nephelometer TSI 3563 have been corrected for angular non idealities (truncation to 7 – 170°, slightly not cosine-weighted distribution of illumination) according to Anderson and Ogren (1998). The equations linking the correction factor and the Angstrom coefficient established for sub-µm particles (Anderson and Ogren, 1998) were used for correcting total scattering, since the median sub-µm mass fraction was 0.67 in Ispra over 2005. This leads to a quite conservative correction (+5-10% for scattering, ca -5% for backscattering). However, the Nephelometer was operated without RH control, and RH inside the Nephelometer was recorded from June 25th only. It was observed that RH in the Nephelometer generally exceed 60% when the outdoor maximum daily temperature is larger than 20°C (95th percentile), which can usually occur from May to Sept. At such a RH, scattering coefficients are 25% larger than in dry conditions, based on calculations accounting for a mean refractive index derived from chemical composition, the Ångstroem coefficient, and the Mie theory (Nessler et al., 2005). Over 2005, corrections for RH were <25 % for 88% of the 24-hr average values.

Atmospheric particle absorption coefficients were derived from the Aethalometer AE-31 data corrected for the shadowing effect when Nephelometer data were available, and for the multiple scattering occurring on/into the Aethalometer filter according to Schmid et al. (2006). The correction factors we used were 3.6, 3.65 and 3.95 for blue, green and red light, respectively. Corrections for the shadowing effect were generally < 20% (90th percentile). Therefore, possible biases in scattering coefficient determination are not expected to affect the determination of the aerosol absorption coefficient significantly. The uncertainty of the multiple scattering correction factor may introduce a much larger uncertainty in the aerosol absorption coefficient values, since correction factors ranging from 2 to 4 have been proposed (Weingartner et al., 2003; Arnott et al., 2005).
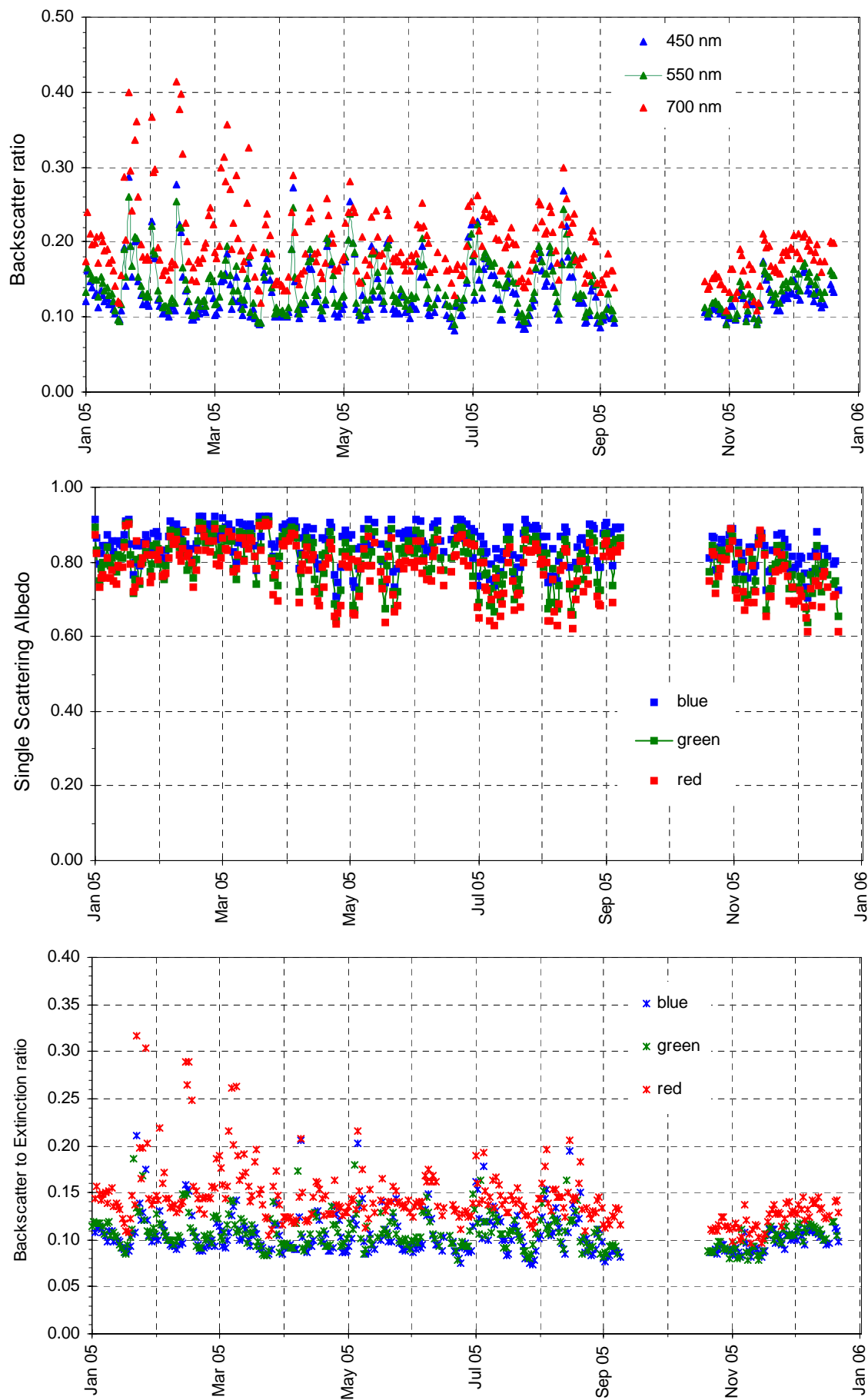
Fig 25: aerosol 24-hr average backscatter to total scatter ratio, single scattering albedo, and backscatter to extinction ratio at three wavelengths corresponding to blue, green and red (RH generally < 40%).

It should be noted that the use of the correction coefficients proposed by Schmid et al. (2006) leads to aerosol absorption coefficients equal to 81% of the PSAP-matched aerosol absorption coefficients calculated from the regression found in the Aethalometer manual (version 2003.04, p.11): PSAP abs. coef. [Mm^{-1}] = 10.78 EBC [μg m^{-3}].

Both scattering and absorption coefficients follow seasonal variations (Fig. 24) in line with PM mass variations, mainly controlled by pollutant dispersion rates.

The backscatter / total scatter ratio generally ranged from ca. 10 to ca. 20%, except for red light during the first part of the year (Fig. 25). The 24 hr averaged single scattering albedo for green light (at RH generally <40%) ranged from 0.64 to 0.91 (annual average 0.80). The aerosol extinction coefficient was calculated as the sum of the scattering and absorption coefficients.

The aerosol extinction coefficient and particle mass or volume concentrations are well correlated, in spite of a few obvious outliers (Fig. 26). The slope of the regression between extinction and mass shows that the extinction mass efficiency is on average 4.2 m^2 g^{-1}, to be compared with 4.6 m^2 g^{-1}, the value calculated based on the aerosol mean chemical composition over 2005, and mass cross section coefficients for the various constituents found in the literature (Table 3).
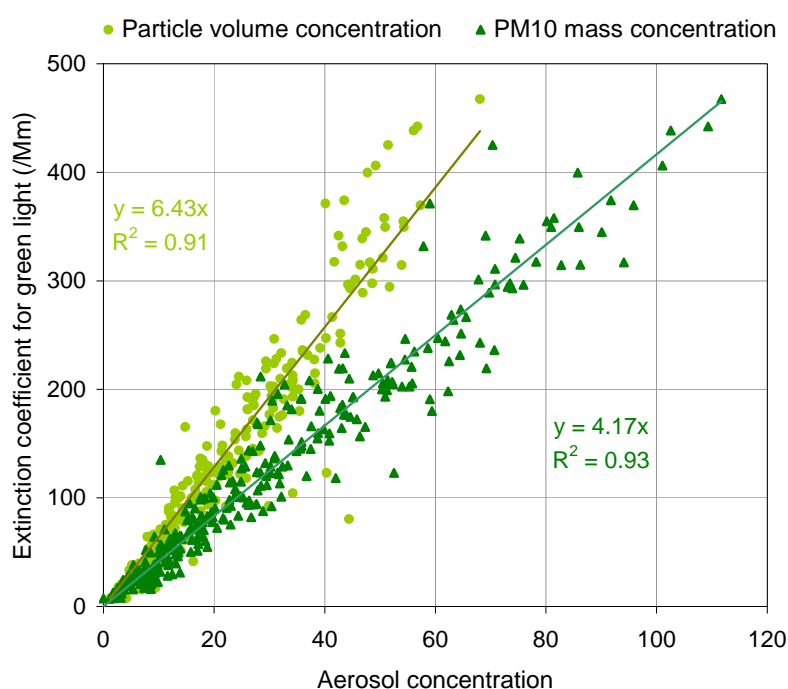

Fig. 26: regressions between the aerosol extinction coefficient and atmospheric particle mass and volume concentrations.

Table 3:mean aerosol chemical composition (PM10) in 2005 and extinction efficiency

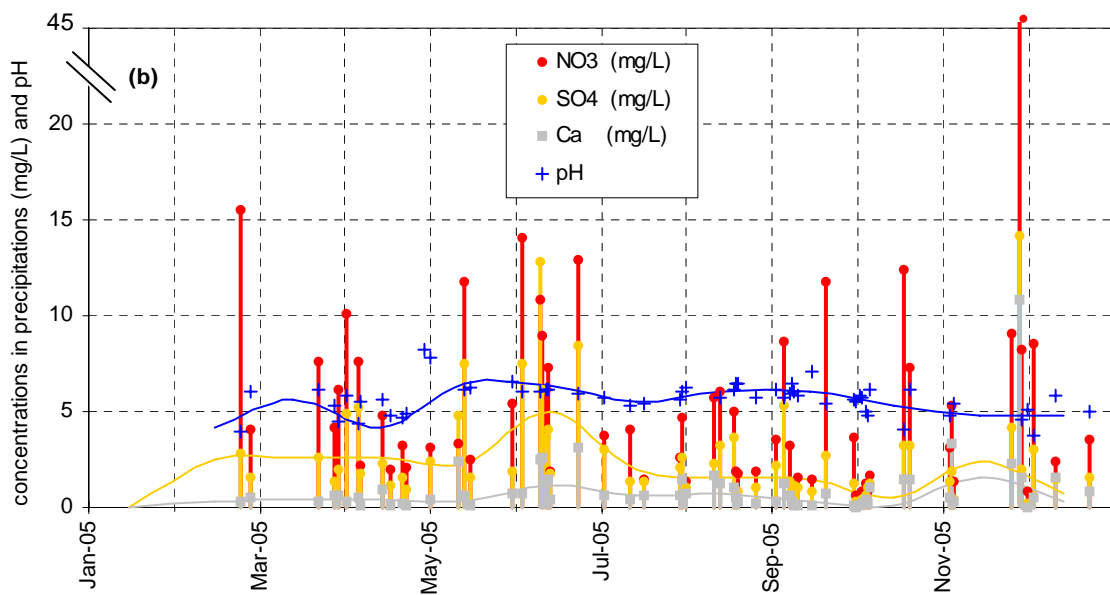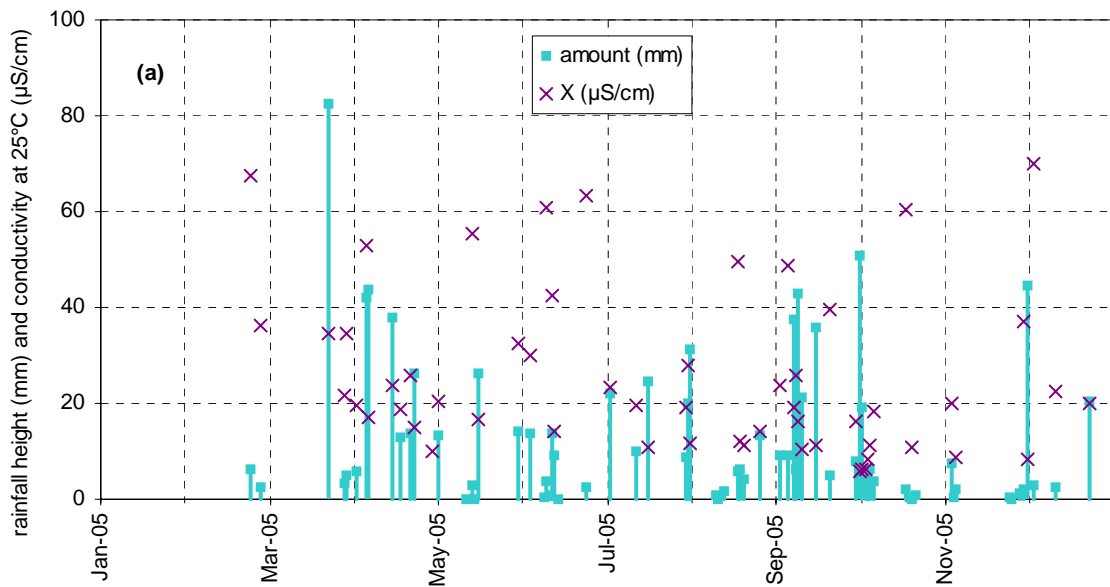|	PM10 comp. (%) in 2005	σ_{ext} (m²/g)	Reference (for σ_{ext})
"sea salt"	3	1.3	Hess et al., 1998
ammonium nitrate and sulfate	35	5.0	Kiehl et al., 2000
organic matter	47	3.6	Cooke et al., 1999
black carbon	10	11	Cooke et al., 1999
dust	4	0.6	Hess et al., 1998
total	100	4.6	

Fig. 27: (a) precipitation amount, conductivity and (b) concentrations of 3 main precipitation components and pH recorded in 2005 (bars and crosses) and over the 1990-1999 period (lines)
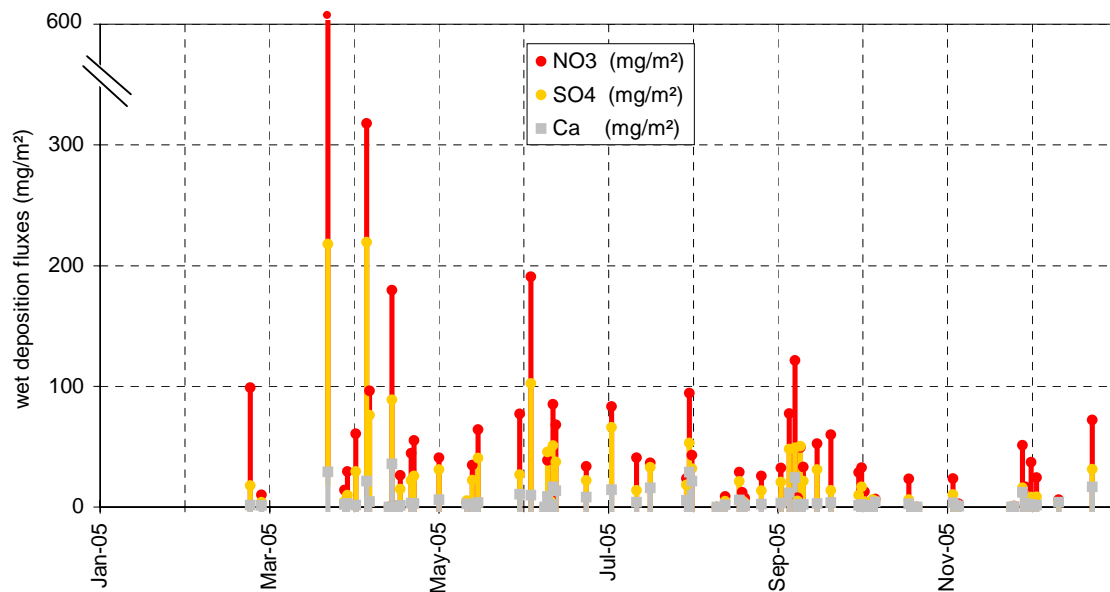

Fig. 28: wet deposition fluxes of 3 main components in rain water for 2005

Precipitation phase

In 2005, 68 precipitation samples were collected, among which 4 snow and 1 rain + snow samples. The precipitation height of the collected events ranged from 0.1 to 82 mm (Fig. 27a), for a total of 881 mm (vs. 831 mm observed at Bd. 51).

The ranges of concentrations measured in these samples are indicated in Table 4. Weighed average SO_4^{2-} and H^+ concentrations were significantly smaller in 2005 compared to the 1990-1999 average, whereas the concentrations of other components was comparable to the 1990-1999 period, or even larger (case of NH_4^+).

Precipitation samples collected in 2005 were all acidic but one (3 May 2005), for which there was no clear indication of a Saharan dust transport episode though (Fig. 27b).

Table 4: parameters relative to the precipitation samples collected in 2005

	pH	cond. $\mu S\ cm^{-1}$	Cl^- $mg\ l^{-1}$	NO_3^- $mg\ l^{-1}$	SO_4^{2-} $mg\ l^{-1}$	Na^+ $mg\ l^{-1}$	NH_4^+ $mg\ l^{-1}$	K^+ $mg\ l^{-1}$	Mg^{2+} $mg\ l^{-1}$	Ca^{2+} $Mg\ l^{-1}$
2005 average	4.75	22.13	0.42	3.85	1.99	0.30	1.88	0.11	0.05	0.46
min	3.79	5.93	0.13	0.64	0.19	0.04	0.05	0.01	0.01	0.04
max	7.77	203	20.4	45.4	14.4	10.1	105.8	4.69	1.63	10.9
1990-1999 av.	4.40	24.86	0.44	3.94	3.07	0.23	1.25	0.09	0.06	0.45

Wet deposition occurred evenly from late February to late December (Fig. 28), with 2 main events on March 24th and Apr. 7th. The annual wet deposition flux of the main acidifying and eutrophying species were 1.8, 3.4, and 1.7 g m^{-2} for SO_4^{2-}, NO_3^-, and NH_4^+, respectively. These fluxes are smaller than in 2004, and comparable to yr 2003, except for NH_4^+ for which 2005 flux was as large as 2004's, and much larger than in 2003 (see Fig. 29-31).
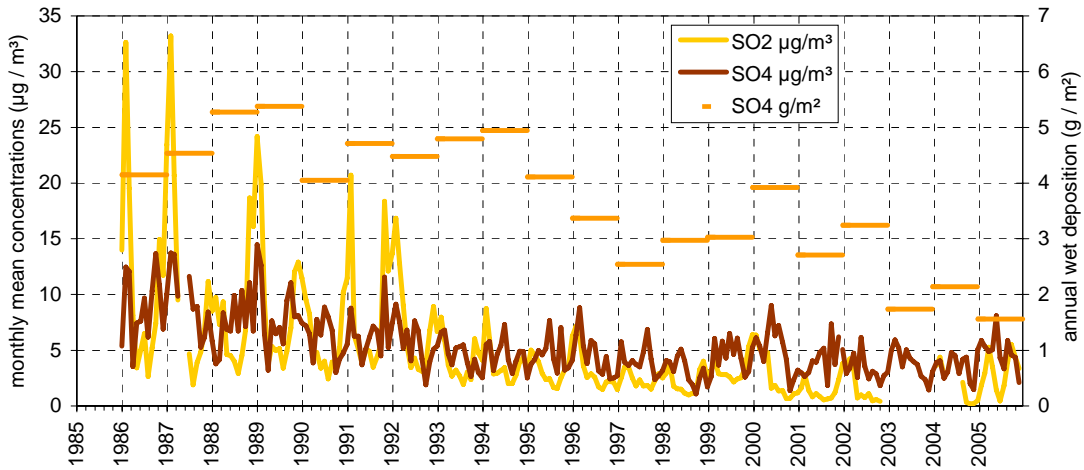
Fig. 29: oxidized sulfur species monthly mean concentrations and yearly wet deposition
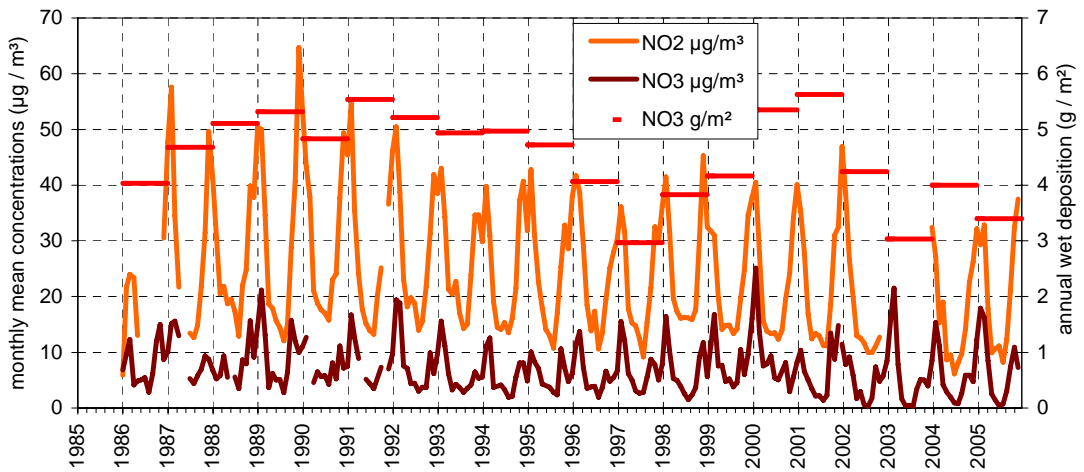

Fig. 30: oxidized nitrogen species monthly mean concentrations and yearly wet deposition
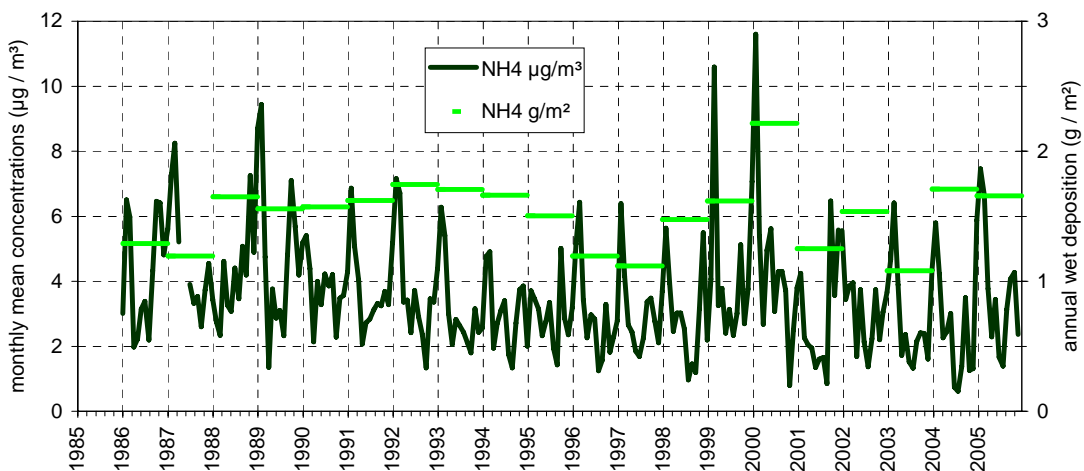

Fig. 31: reduced nitrogen species monthly mean concentration and yearly wet deposition

Results of year 2005 in relation with 2 decades of monitoring activities

Sulfur and nitrogen compounds

Both winter maxima and summer minima monthly mean concentrations of sulfur dioxide (SO_2) decreased by a factor >5 over the past 20 years (Fig. 29). The standard SO_2 monitor was no more suited from 2002 (concentrations often below detection limit during summertime 2002, large noise in summer 2004), and was therefore replaced with a trace level instrument from Dec. 2004. Particulate SO_4^{2-} showed also a clear decreasing trend from 1986 to 1998 (factor 3), but seems to stabilize around the mean value for the 90's since then.. It should kept in mind that SO_4^{2-} concentrations were measured in PM10 from 2002, whereas it was measured in TSP (Total Suspended Particulate) from 1986 to 2001. However, simultaneous sampling of PM10 and TSP over 14 months showed that SO_4^{2-} in PM10 is generally less than 5% lower than in TSP. SO_4^{2-} wet deposition reached its historical minimum in 2005 (much dryer than usual year), and the value observed in 2003 and 2004 were both close to this historical minimum. These data show that locally produced SO_2 decreased much more than possibly long-range transported SO_4^{2-} over the past 20 years.

Monthly mean concentrations of nitrogen dioxide (NO_2) do not show such a pronounced decreasing trend over the last 2 decades (Fig. 30). Wintertime NO_2 maxima indeed remained quite constant over 1993-2002, and did not reflect the 30% abatement in NOx emissions over the 1992-2000 period (Perrino and Putaud, 2003). However, NO_2 concentrations observed in 2004 and 2005 were the lowest since 1987. Particulate NO_3^- annual mean concentration reached its minimum in 2002, but concentrations observed in 2003 - 2005 were comparable to values observed in the nid-90's, mainly due to higher wintertime values. It should be noted that since October 2000, NO_3^- is measured from quartz fiber filters, which are known to lose NH_4NO_3 at temperatures > 20°C. This might contribute significantly to the fact that NO_3^- summertime minima are particularly low since 2001. Furthermore, NO_3^- was measured from PM10 from 2002, and no more from TSP, as over the 1986 to 2001 period. However, simultaneous sampling of PM10 and TSP over 14 months showed that NO_3^- in PM10 is generally less than 5% lower than in TSP, like SO_4^{2-}.
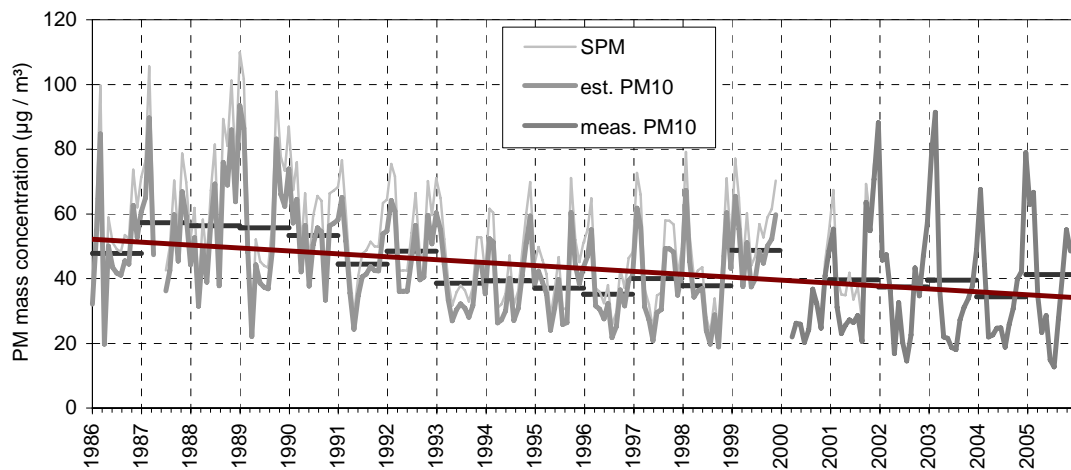
Fig. 32: particulate matter mass concentration monthly and annual averages
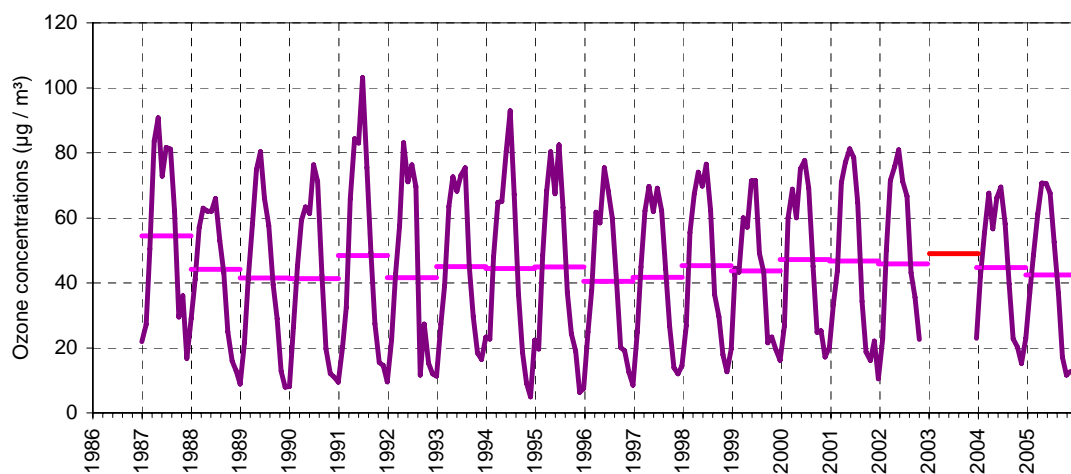

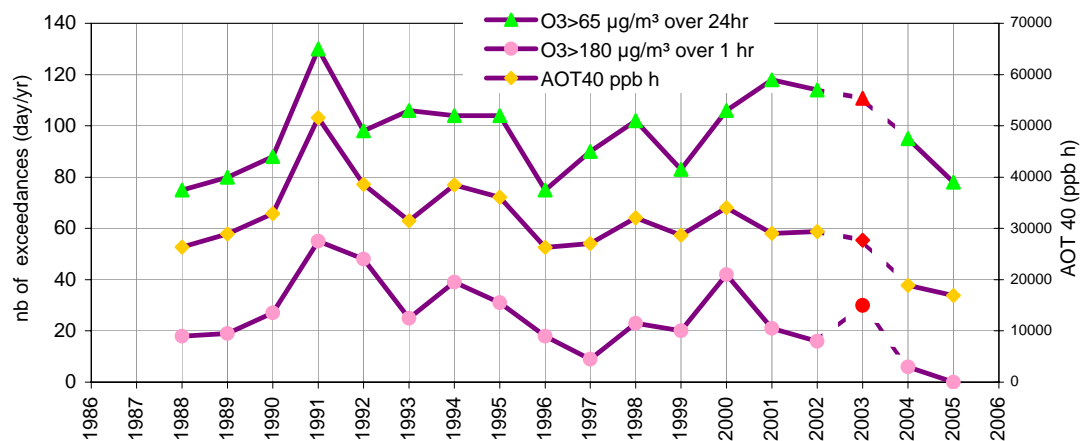*Fig. 33: Ozone yearly and monthly mean concentrations. 2003 data from Malpensa airport.*

Fig. 34: AOT40 values and number of days on which indicated O₃ limit values were reached.

Red symbols indicate estimates based on Malpensa airport data (no data from Ispra in 2003).

NO_3^- wet deposition annual flux observed in 2005 was close (10% higher) to the 1997 historical minimum (at least partially due to a very low precipitation amount in 2005), i.e. much lower than the annual wet deposition fluxes observed over the last 20 years. Monthly mean concentrations of NH_4^+ in the particulate phase appear to decrease over 1986 – 2004 (Fig. 31), specially because summertime minima decreased. There is no clear trend regarding NH_4^+ wintertime maxima. On average, NH_4^+ can neutralize > 85% of the acidity associated with NO_3^- and SO_4^{2-} in the particulate phase. NH_4^+ is also quite well correlated with $NO_3^- + SO_4^{2-}$ in rainwater. NH_4^+ wet deposition was particularly large in 2004 and particularly in 2005, considering the low amount of precipitation over the latter year.

Particulate matter mass

The PM_{10} values observed in 2005 do not confirm the general decreasing trend in PM_{10} observed over the last 2 decades (Fig. 32). Indeed, PM10 concentrations were in 2005 as large as during the 90's, and for the first time since 2000, larger than the annual EU limit of 40 µg/m³ to be reached from 2005. This might be at least partially due to the fact that 2005 was particularly dry. However, a statistical analysis still indicates that PM10 has been decreasing by about 0.5 µg m^{-3} yr^{-1} over 1986-2005. It should be kept in mind that PM10 concentrations were estimated from TSP mass concentration measurements (carried out by weighing at 60% RH and 20°C cellulose acetate filters sampled without any particle size cut-off and "dried" at 60°C before and after sampling) over 1986-2000, based on a comparison between TSP and PM10 over the Oct. 2000 - Dec. 2001 period (R² = 0.93, slope = 0.85).

Ozone

Fig. 33 shows monthly and yearly mean O_3 concentrations observed since 1987. To close the gap due to the data acquisition breakdown in 2003, O_3 data from Malpensa airport have been used to estimate values based on a comparison between Ispra and Malpensa over 2004. No clear trend in O_3 annual mean concentrations can be deduced from the observations over 1987-2005. Indeed, the annual averages observed in 2004 and 2005 are not lower than that observed in 1989 – 1990. However, summertime monthly maxima observed in 2004 – 2005 were among the lowest since 1989. Also, O_3 wintertime minima increased from 1995 to 2001, but decreased from 2004.

Fig. 34 shows that AOT40, the vegetation exposure to above the O_3 threshold of 40 ppb (80 µg/m³) started to decrease again from 2002, as well as the number of days

with a mean O_3 concentration > 65 µg/m³ (vegetation protection limit). The number of days on which the limit value for people information (180 µg/m³ over 1hr) was reached or exceeded also decreased from 2000 (the estimated value for 2003 excepted) and reached 0 for the first time since O_3 was measured in Ispra. The frequency of extreme ozone values clearly decreased since 2000, but the slight decrease in O_3 background values, consistent with decreasing NO_2 concentrations, has still to be confirmed.

Conclusion

Gas phase measurements were carried out throughout 2005 without major gaps. Aerosol sampling on quartz fiber filter for gravimetric and chemical analyses were also performed over the whole year. However, Scheilcher & Schuell filters were abandoned from December 2005 (no more available on the market), and replaced by Whatman QMA filters for this month. We stopped sampling PM_{10} and $PM_{2.5}$ on July 30th, 2005, and started collecting PM_{coarse} and $PM_{2.5}$ with a Partisol dichotomous sampler from July 1st, 2005. Gravimetric analyses at 20% RH led to inconsistent results for months June, July, and August. Also PM_{10} gravimetric measurements at 20% RH were excluded for June. All $PM_{2.5}$ samples were analyzed for carbonaceous components with the new Sunset Lab OCEC instrument, with different thermal protocol for Jan. - Apr. (last step in He at 650°C) and May – Dec. (last step in He at 550°C) yet. The EMEP'2005 intercomparison for rainwater analyses suggests that we might have underestimated NH_4^+ by as much as

35%. However, the ionic balance in both rainwater and aerosol samples demonstrate a perfect agreement between NH_4^+ measurement on the one hand, and $NO_3^- + SO_4^{2-}$ measurements on the other hand. PM_{10} samples collected over Jan. – Apr. 2005 were analyzed both with the old C analyzer RA10M and the new Sunset Lab Instrument (with the last step in He at 650°C). PMcoarse samples were analyzed with the Sunset Lab. Instrument. Particle number size distributions were performed with a DMPS and an APS along the year, except for maintenance periods. The aerosol density d = 1.5, proved *a posteriori* to be consistent with other measurements, was used to convert aerodynamic diameters to mobility equivalent diameters. Using this density value leads to reasonable agreements between the DMSP and APS size distribution measurements. Aerosol scattering and absorption coefficients were derived from Nephelometer and Aethalometer measurements, respectively, applying state-of-the-art corrections to these measurements. However, these data were not normalized to a standard relative humidity. It should be noticed that the extinction-to-mass ratio dropped from 4.9 to 4.2 m^2 g^{-1} from 2004 to 2005, mainly due to smaller extinction coefficients in 2005. Both these estimates are consistent with the value that can be calculated from the mean PM_{10} chemical composition (ca. 4.5 m^2 g^{-1}).

The data listed by EMEP as core parameters have been reported to NILU (http://www.nilu.no/projects/ccc/). Most others are available from http://carbodat1.jrc.it/ccu/down1/emepq_New.php.

Sulfur dioxide (SO_2), carbon monoxide (CO), and nitrogen dioxide (NO_2) presented seasonal variations (low concentrations in summer, higher concentrations in winter) comparable to the other years, and consistent seasonal changes in pollutant dispersion. O_3 maximum concentrations were observed in June-July, in line with the seasonal variations in solar irradiation. The long-term trends in SO_2 concentrations (decreasing), and summertime NO_2 concentrations (decreasing since 1998) were not infirmed by the measurements performed in 2005. Wintertime NO_2 concentrations were also smaller in 2005 compared to average. The decreasing trend in O_3 extreme value frequency was also confirmed in 2005, and for the first time since 1986, no exceedances of the 1hr O_3 limit value of 180 μg/m³ was observed. However, the slight decrease in average O_3 concentrations observed since 2000 (2003 excluded) still has to be confirmed.

Gravimetric measurements operated at 20% and 50% RH confirmed that PM mass measured at 20% RH was consistently 7-9% lower than PM mass measured at 50% RH. The PM2.5 / PM10 mass concentration ratio observed at JRC-Ispra in 2005 was 0.78. The full chemical characterization of PM10 (main inorganic ions, organic carbon, black carbon and estimated mineral dust) segregated in two size fractions showed that particulate organic matter (POM) is generally by far the main component of both the fine (<2.5 μm) and coarse (>2.5 μm) aerosol size fractions. However, there is a clear enhancement of the secondary inorganic component contribution when shifting from cleaner (PM_{10}<50μg/m³) to more polluted periods (PM_{10}>50μg/m³). It should be noted that with the assumption used to estimate POM and dust from organic carbon (OC) and Ca^{2+}, respectively, the whole PM mass concentration could be explained in 2005, in contrast to what occurred for the previous years. PM_{10} annual averaged exceeded the EU limit value (50μg/m³) for the first time in 2005 since 2000. This might be at least partially due to the fact that 2005 was a particularly dry year (less precipitation events and volume than usual). However, the long term time series still suggests a PM10 mass concentration decrease of 0.5 $\mu g \ m^{-3} \ yr^{-1}$ over the last 2 decades.

Average particle number was close to 10000 cm^{-3}. Particle number size distributions were generally slightly bimodal, with a submicron mode at ca. 100 nm (dry) and a coarse mode around 2 μm. Atmospheric aerosol scattering and absorption coefficients at various wavelengths were derived from Nephelometer and Aethalometer measurements at not controlled (but generally lower than ambient, except in summer) relative humidity. The single scattering albedo (at RH generally < 40%) was 0.80 over 2005.

The aerosol extensive parameters measured at JRC-Ispra (at ground level) all follow a comparable seasonal trend with minima in winter. These parameters are generally well correlated and lead to reasonable degrees of chemical, physical, and optical closures.

Except for SO_4^{2-} and H^+, rainwater component concentrations were not smaller in 2005 compared to the 1990-1999 average, and even larger in the case of NH_4^+. This may be due to the fact that the amount of precipitation was particularly low in 2005. Indeed, the wet deposition fluxes of the main acidifying and eutophying species were comparable to the previous years. No clear event of "desert dust wet deposition" was detected in 2005.

References

Anderson, T.L., and Ogren, J.A., Determining aerosol radiative properties using the TSI3563 integrating nephelometer, *Aerosol Sci. Technol.*, **29**, 57-69, 1998.

Arnott, W.P., Hamasha, K., Moosmüller, H., Sheridan, P.J., and Ogren, J.A., Towards aerosol light-absorption measurements with a 7-wavelength aethalometer, …, *Aerosol Sci. Technol.*, **39**, 17-29, 2005.

Burch, D. E.; Gates, F. J.; Pembrook, J. D., Ambient carbon monoxide monitor. Research Triangle Park, NC: U.S. Environmental Protection Agency, Environmental Sciences Research Laboratory; report no. EPA-600/2-76-210, 1976.

Cooke, W.F., Liousse, C., Cachier, H., and Feichter, J., Construction of a 1x1°fossil fuel emission data set for carbonaceous aerosol and implementation and radiative impact in the ECHAM4 model , *J Geophys. Res.*, **104**; 22,137-22,1999.

Hess, M., Koepke, P. Schult, I., Optical Properties of Aerosols and Clouds: The Software Package OPAC, *Bull. of Am. Meteorol. Soc.*, **79**; 831-844, 1998.

Kiehl, J. T., Schneider, T. L., Rasch, P. J., Barth, M. C., Wong, J., Radiative forcing due to sulfate aerosols from simulations with the National Center for Atmospheric Research Community Climate Model, Version 3 (Paper 1999JD900495), *J. Geophys. Res.,* **105**; 1441-1458, 2000.

Nessler, R., Weingartner, E., and Baltensperger, U., Adaptation of dry nephelometer measurementsto ambient conditions at the Jungfraujoch, Environ. Sci. Technol., 39, 7, 2219-2228, 2005.

Perrino, C., and Putaud, J.P., Assessment of the EMEP measurement and modelling work in Europe from 1977 until Today: national contribution of Italy, *EUR* **20979** EN, 2003.

Schmid, O., et al., Spectral light absorption by ambient aerosols influenced by biomass burning in the Amazon Basin I: comparison and field calibration of absorption measurements techniques, *Atmos. Chem. Phys.*, **6**, 3443-3462, 2006.

Weingartner, E., Saathoff, H., Schnaiter, M., Streit, N., Bitnar, B., and Baltensperger, U., Absorption of light by soot particles: determination of the absorption coefficient by means of aethalometers, *J. Aerosol Sci.*, **34**, 1445-1463, 2003.

European Commission

Abstract

The aim of the JRC-Ispra station for atmospheric research (45°49'N, 8°38'E) is to monitor atmospheric parameters (pollutant concentrations and fluxes, atmospheric particle chemical composition, number size distribution and optical properties) to contribute in assessing the impact of European policies on air pollution and climate change. The station has been operated continuously since November 1985, with a gap in gas phase data due to a severe breakdown of the data acquisition system in 2003 though.

The measurements performed in 2005 led to annual averages of ca. 43 μg m^{-3} O_3, 4 μg m^{-3} SO_2, 16 μg m^{-3} NO_2, 0.8 mg m^{-3} CO and 41 μg m^{-3} PM10. Carbonaceous species (organic matter plus elemental carbon) are the main constituents of both PM10 and PM2.5 (> 50%) followed by $(NH_4)_2SO_4$ and NH_4NO_3 (a bit less than 20% each). The measurements confirmed the seasonal variations observed over the previous years, mainly driven by meteorology rather than by changes in emissions. Aerosol physical and optical properties were measured from 2004. The average particle number (from 6 nm to 10 μm) was about 10000 cm^{-3} in 2005. The mean (close to dry) aerosol single scattering albedo (a key parameter for determining the aerosol direct radiative forcing) was 0.80.

Long-term trends (over 20 years) show decreases in sulfur concentrations and deposition, and in extreme ozone value occurrence frequency. The decreasing trends in nitrogen oxides, reduced nitrogen species, and PM concentrations are much less marked.

The mission of the JRC is to provide customer-driven scientific and technical support for the conception, development, implementation and monitoring of EU policies. As a service of the European Commission, the JRC functions as a reference centre of science and technology for the Union. Close to the policy-making process, it serves the common interest of the Member States, while being independent of special interests, whether private or national.